PONTIFICIA UNIVERSIDAD CATOLICA DE CHILE
ESCUELA DE INGENIERIA

SIMPLIFIED PROBABILISTIC EVALUATION OF THE SEISMIC PERFORMANCE OF THREE PILE-SUPPORTED BRIDGES AFFECTED BY LIQUEFACTION

DANIEL JAVIER ALEJANDRO GONZALEZ PAIZ

Thesis submitted to the Office of Research and Graduate Studies
in partial fulfillment of the requirements for the degree of
Master of Science in Engineering

Advisor:
CHRISTIAN ALFONSO LEDEZMA ARAYA

Santiago de Chile, Diciembre 2014

PONTIFICIA UNIVERSIDAD CATOLICA DE CHILE
ESCUELA DE INGENIERIA

SIMPLIFIED PROBABILISTIC EVALUATION OF THE SEISMIC PERFORMANCE OF THREE PILE-SUPPORTED BRIDGES AFFECTED BY LIQUEFACTION

DANIEL JAVIER ALEJANDRO GONZALEZ PAIZ

Members of the Committee:
CHRISTIAN ALFONSO LEDEZMA ARAYA
ESTEBAN PATRICIO SAEZ ROBERT
GONZALO ANDRÉS MONTALVA ALVARADO
JOSÉ FRANCISCO MUÑOZ PARDO

Thesis submitted to the Office of Research and Graduate Studies
in partial fulfillment of the requirements for the degree of
Master of Science in Engineering

Santiago de Chile, Diciembre 2014

*A Dios por todas sus bendiciones,
en memoria de mi madre, a mi
familia y a mi novia, quienes
creyeron en mi y me apoyaron todo
el tiempo*

ACKNOWLEDGEMENTS

First I want to thank God for all the blessings he has given me, is He who gives me the strength to go on. To my family that always supported, believed, and motivated me week to week to complete this goal even when the road seem adverse, I love you all. In memory of my mother who was my example of struggle and strength. To my girlfriend for her patience, love, support, and understanding, I don't know what I would do without you.

To my advisor, professor Christian Ledezma, for his disposition, recommendations, for sharing ideas, and for his guidance throughout the entire research process. To the other professors in the Department of Structural and Geotechnical Engineering, with whom I took courses or consulted during my research, for sharing their vast knowledge that helped me grow as a student and as an engineer.

To my mates of the structural and geotechnical engineering department, for all those talks at lunch time or late at night before returning home, for those summers and winters, where even dead of heat or cold, we supported one another to complete our researches. Thanks for making me part of the group and for your friendship.

Finally, thanks to the Organization of American States (OAS) for the granted scholarship to carry out postgraduate studies outside of Guatemala, and also to the sponsorship of Fondecyt proyect 11110125 that allowed to develop and complete this research.

TABLE OF CONTENTS

LIST OF FIGURES

LIST OF TABLES

ABSTRACT

The 2010 M8.8 Maule earthquake caused damage and partial collapse on various pile-supported bridges along the coast of Chile. These damages were probably due to effects of liquefaction-induced lateral and vertical ground displacements, which often cause large ground deformation that impose additional loads on the pile foundations. In this thesis the seismic performance of three bridges will be analyzed, based on the residual lateral displacement of the abutments and/or piers of each bridge, using a simplified methodology. The analyzed bridges were: Juan Pablo II Bridge, Llacolén Bridge, and Mataquito Bridge. These bridges were selected not only because of the clear evidence of liquefaction at their respective locations, but also because their seismic behavior was very different between them. The analysis was carried out using two approaches, a liquefaction triggering evaluation along with the *"pile-pinning"* concept, and a performance-based probabilistic approach. Liquefaction susceptibility was evaluated using SPT-profiles, which were provided by the Ministry of Public Works (MOP in Spanish). The analytical method mainly consists of: identification of liquefiable layers, slope stability analysis of the abutment and/or pier, estimation of lateral ground displacement, and a pile response analysis due to lateral displacement. The probabilistic method was evaluated using a spreadsheet provided by the authors of this method. Reasonable to good agreement between these estimates and the actual observed damages of these bridges was found. Comparing the obtained results, there is no clear evidence that one method is more accurate than another, because both methods deliver conservative ranges of expected lateral displacements, especially the probabilistic method.

Keywords: 2010 Maule earthquake, Liquefaction, Lateral Spreading, Pile Foundation, Bridges

RESUMEN

El terremoto de Maule del 2010 de magnitud M8.8 causó daños y colapsos parciales en varios puentes apoyados sobre pilotes a lo largo de la costa de Chile. Estos daños fueron probablemente debido a efectos de desplazamiento lateral y asentamientos inducidos por licuación, los que generalmente causan grandes deformaciones en el suelo y a la vez imponen cargas adicionales en los pilotes de las fundaciones. En esta tesis se analizará el desempeño sísmico de tres puentes, basandose en el desplazamiento lateral residual de los estribos y/o cepas de cada puente, utilizando una metodologia simplificada. Los puentes analizados son: Juan Pablo II, Llacolén y Mataquito. Dichos puentes fueron seleccionados no solo por la clara evidencia de licuación en sus respectivas ubicaciones, sino también porque su comportamiento sísmico fue muy distinto entre ellos. El análisis se llevó a cabo utilizando dos enfoques, una evaluación de activación de licuación en conjunto con el concepto de *"pile-pinning"* y una evaluación probabilística enfocada al desempeño. Para la evaluación de susceptibilidad de licuación se utilizaron perfiles de Penetración Standart (SPT), los cuales fueron proporcionados por el Ministerio de Obras Públicas (MOP). El método analitico consiste principalmente en: identificación de capas licuables, análisis de estabilidad del estribo y/o cepa, estimación del máximo desplazamiento lateral del suelo y análisis de respuesta de los pilotes de la fundación ante el desplazamiento lateral. El método probabilistico se evaluó utilizando una hoja de cálculo proporcionada por los autores de este método. Se encontró que existe una correlación razonable buena entre las estimaciones de desplazamiento lateral obtenidas y el daño observado en los puentes. Comparando los resultados obtenidos, no existe clara evidencia de que un método sea mas preciso que otro, pues ambos métodos entregan rangos de desplazamiento conservadores, sobre todo el método probabilistico.

Palabras Claves: Terremoto de Maule del 2010, Licuación, Desplazamiento Lateral, Fundaciones sobre Pilotes, Puentes

1. INTRODUCTION

1.1. Problem Statement

1.1.1. Background

In February 27, 2010 the M_w = 8.8 Maule earthquake caused significant damages in Chile's infrastructure, including a number of bridges, railroads, roads, and life-line structures (Bray & Frost, 2010). The affected area covered approximately 600 km along the coast by 100 km wide, an it included several regions and metropolitan areas. An important highway that runs in the north-south direction, and connects these two cities (Route 5) is crossed by a number of rivers that run mainly from east to west.

Most of the bridge structures along Route 5 performed well during the earthquake. The earthquake strong shaking triggered liquefaction and lateral spreading, particularly near rivers, streams, and along the coastline. The alluvial sediments and long duration of shaking, most likely contributed to the observed liquefaction in several bridge locations. Based on strong motion records, ground shaking lasted for more than two minutes in the Santiago area. For loose, saturated, granular soils long-duration events impose a significant number of strain cycles, which also generates excess pore pressures. Although some of the observed damage was severe, the overall seismic performance of bridge decks and superstructures was quite good. The Ministry of Public Works (MOP in Spanish) reported that only about 5.7% of bridges, underpasses, and overpasses suffered different levels of earthquake-induced damage (MOP, 2010).

The Bío-Bío River is the second longest river in Chile and it is also the widest, with an average width of 1 km, and a width of more than 2 km prior to discharging into the ocean. Close to the Pacific Ocean, the river traverses the metropolitan area of Concepción. In Concepción, the river is crossed by five bridges: Juan Pablo II Bridge (opened in 1974), Llacolén Bridge (2000), La Mochita Bridge (2005), Puente Viejo Bridge (1942) and Bío-Bío Railroad Bridge (1889). During the February 27 M_w = 8.8 earthquake all of these bridges experienced different levels of structural damage, compromising normal business activities in the region. The most common geotechnical failure mechanisms observed at these bridges were liquefaction-induced lateral spreading that occurred along both shores of the Bío-Bío River, and settlement in some bridge bents. Most of the damage occurred at Llacolén and Juan Pablo II bridges. Similarly, the Mataquito Bridge (near Iloca) was also subjected to extensive lateral spreading effects. The seismic performance of these bridges was very different, ranging from little foundation deformations causing negligible to small damages that did not affect the bridge structure, to moderate foundation deformations that caused large distributed damage that even lead to bridge closure.

1.1.2. Motivation

The analysis of ground failure case studies is one of the most important sources of feedback for geotechnical earthquake engineering, and it has lead to advances in this area. Concepción was selected as the main area of interest because of clear evidence of liquefaction, short distance to the epicenter $R \approx$100 km (62 miles), and different performance of the bridges that cross the Bío-Bío River, more specifically Llacolén and Juan Pablo II bridges. Liquefaction triggering and its consequences such as lateral spreading and ground settlement, caused damages that affected the bridge's decks and superstructure which lead to closure, compromising local transportation and causing logistical problems to treat the emergency. A major earthquake, like the M8.8 Maule, gives the opportunity to check the accuracy of current methods and procedures on the estimation of lateral displacements due to liquefaction, when compared against in-situ measurements. These comparisons are useful, for example, to validate current methods, to enhance the available information about lateral spreading, and to evaluate current local design standards.

The methodology exposed herein evaluates the relationship between the residual lateral displacement and the observed damage in the bridge structure. Based on the residual lateral displacements, key observations can be made about the seismic performance of the bridges. This methodology makes use of the well-known liquefaction triggering procedure by Youd et al. (2001), in combination with common engineering practice software, and the *"pile-pinning"* effect, to get estimates of the residual lateral displacements. In addition, the damage levels proposed by Ledezma & Bray (2010), are used to give a qualitative description of the bridges seismic performance.

The use of this simplified evaluation of the seismic performance of pile-supported bridges, which is based on readily available structural, geotechnical, and seismological information, gives design engineers a tool that would quickly help them check projects in a preliminary design phase. The results from these analyses provide an adequate estimation of expected lateral displacements in bridge abutments or intermediate bents, to evaluate if the displacements are tolerable or not.

1.2. Objectives

The main objective of this research is to evaluate the seismic performance of three pile-supported bridges affected by laterally spreading ground triggered by liquefaction. This seismic performance evaluation is based on the residual lateral displacement of bridge abutments and/or bents, where the effects of liquefaction-induced lateral spreading are evaluated based on the design procedure proposed in the MCEER/ATC-49-1 report, a guideline for the seismic design of bridges (ATC/MCEER Joint Venture, 2003). Additionally, the seismic performance is also evaluated using a performance-based simplified probabilistic analysis (Ledezma & Bray, 2010).

The specific objectives are:

1. To verify that the current methods used to evaluate liquefaction susceptibility and effects, correlate well with the observed damage.
2. To determine, if the residual lateral displacements can explain the structural damage observed at each bridge.
3. To determine, from a probabilistic method, the residual lateral displacements at each bridge and the associated expected level of damage.
4. To compare the results of these two methods, analytical and probabilistic, and assess whether these methods agree or not.

1.3. Literature Review

1.3.1. Liquefaction Susceptibility

Liquefaction is defined as the transformation of a granular material from a solid to a liquefied state as a consequence of increased pore-water pressure and reduced effective stress (Marcuson, 1978). Also soil liquefaction is known as a phenomenon in which soil loses much of its strength or stiffness, soil particles re-arrange to a denser state under a stress perturbation, causing excess pore-water pressure development because of insufficient time for the displaced water to escape (Medina, 2012). The term liquefaction also refers to the phenomena of seismic generation of large pore-water pressures and consequent softening of granular soils (Youd et al., 2001). Based on these definitions, for liquefaction to develop, three elements are needed: loose to moderately dense saturated granular soils, water presence, and cyclic loading (e.g.: earthquake shaking, vibrations). Since liquefaction is one of the most dramatic causes of damage to structures during earthquakes, the evaluation of soil liquefaction resistance is an important aspect of geotechnical engineering practice.

In the summary report by Youd et al. (2001), and following the original work by Seed & Idriss (1971), the authors indicate that two variables are required to evaluate the liquefaction triggering of soils. The first one is the seismic demand on the soil layer expressed in terms of the Cyclic Stress Ratio (CSR); and the second one is the capacity of the soil to resist liquefaction, expressed in terms of the Cyclic Resistance Ratio (CRR). The CSR is the ratio between the average shear stress during shaking, and the effective vertical overburden stress. The parameters used to calculate this value are taken from the in-situ soil conditions and the acceleration record of the earthquake of interest. On the other hand, the value of CRR is directly associated with the in-situ stress-state of the soil. Unfortunately, this stress-state usually cannot be reestablished in the laboratory, and samples of granular soils obtained in the field are usually too disturbed. To avoid the difficulties associated with sampling and laboratory testing, field tests have become commonly used for liquefaction assessment. One of these tests is the Standard Penetration Test (SPT).

This test is carried out in a borehole, by driving a standard “split spoon” sampler using repeated blows of a 63.5kg (140 lb.) hammer falling through 762mm (30 in.). The hammer is operated at the top of the borehole, and is connected to the split spoon by rods. The split spoon is lowered to the bottom of the hole, and is then driven a distance of 450mm (18 in.), and the blows are counted. The penetration resistance (N) is the number of blows required to drive the split spoon for the last 300mm (1 ft) of penetration.

The Standard Penetration Test (SPT) is probably the most used field test for sampling and soil characterization. In Chile, the Ministry of Public Works (MOP in Spanish) has SPT data from various bridge sites, so this research was based on SPT procedures for soil liquefaction assessment.

Cetin et al. (2004) presented new probabilistic and deterministic relationships for assessing the likelihood of liquefaction triggering, also using SPT data. The resulting relationships provide reduced uncertainty, and they also proposed new magnitude scaling factors, adjustments for fines content, and corrections for overburden stress.

More recently Idriss & Boulanger (2006) presented a series of recommendations and procedures based on field tests, which included an update for the semi-empirical field-based procedures that are used to evaluate the liquefaction potential of cohesionless soils during earthquakes. Also, based on this re-evaluation, they presented revised SPT-based and CPT-based liquefaction correlations for cohesionless soils.

1.3.2. Liquefaction Effects of the 2010 Maule earthquake

The February 27, 2010 M_w = 8.8 Maule earthquake triggered liquefaction over a large area of Chile, particularly near rivers, streams, and along the coastline of the country. The widespread alluvial sediments and long duration of shaking most likely contributed to the large number of observations of liquefaction. The geotechnical report of Verdugo & Peters (2010) presented analyses of SPT profiles from Juan Pablo II Bridge and Llacolén Bridge as part of the preliminary draft for the construction of Chacabuco Bridge. After performing a liquefaction susceptibility evaluation on these SPT profiles, it was determined that for the Juan Pablo II case, liquefiable and non-liquefiable soil layers were intercalated. Also, the observed settlements along the bridge can be explained because the soil beneath several bents liquefied. For the Llacolén Bridge, liquefiable layers were mainly located in the first 5 m, unlike the Juan Pablo II Bridge the pile's tip were located in dense sands, which explains the small settlements and displacements when compared to the latter.

The article by Ledezma et al. (2012) describes the effects that ground failure had on a number of bridges, roadway embankments, and railroads during this major earthquake. It was concluded that liquefaction occurred primarily on sandy deposits along the rivers that run in the east-west direction across central Chile, and that liquefaction of these soils resulted in moderate-to-severe damage to many bridges and other transportation infrastructure. The post-earthquake edited report from the Geotechnical Extreme Events Reconnaissance (GEER) teams (Bray & Frost, 2010), provided additional descriptions of ground failures and damages in several other bridges, roads, railroads and lifelines systems. These documents were the base for selecting the three bridges presented in this thesis.

Consequences of liquefaction included approach fill deformations, ground settlement and lateral spreading. The latter was probably the main reason behind most of the damage in bridges near the epicenter of the earthquake. Bridge decks unseated, rotated and shifted at various bridges as consequence of strong shaking and lateral displacement. While there were isolated cases of embankment fill failures resulting in the closure of roadways, patches of gravel were quickly placed after the earthquake to compensate for settlement of bridge approach fills.

In the Liquefaction Study Report No. MCEER/ATC-49-1 edited by ATC/MCEER Joint Venture (2003), which presents guidelines for the seismic design of bridges, a design approach for the effects of liquefaction-induced lateral spreading on pile-supported bridges is proposed. Four basic elements are involved in this design approach: (1) stability analysis, (2) Newmark sliding block analysis, (3) assessments of the passive force that can ultimately develop ahead of a pile or foundation as soil movement occurs, and (4) assessment of the likely plastic mechanisms that may develop in the foundations and substructure. The rationale behind this approach is to determine the likely magnitude of residual lateral soil movement and assess the structure's ability to accommodate this movement and/or to potentially limit it. It is also mentioned that available software (e.g., LPile (Ensoft, 2013)) can provide useful information for the design of foundations resisting the effects of lateral soil movements.

An example of the impact of lateral spreading on pile foundations can be seen in the technical note by Phanikanth et al. (2012), where they studied the behavior of single piles in liquefied deposits under lateral loads (e.g., inertial loads and lateral spreading) focusing on the evaluation of the bending moments along the piles. The pile response in liquefied soils was significantly amplified when compared against the non-liquefied case, and the amplification in peak pile-bending moments was as high as 2.5. Also, the thickness of the liquefied layer had a significant influence on the soil-pile response. For example, the maximum pile-bending moment occurs at the interface of the liquefied and non-liquefied layers.

1.3.3. Bridge Performance Evaluation

A widely used method to evaluate the seismic performance of pile foundations affected by lateral spreading, is to analyze the piles using a Beam on Nonlinear Winkler Foundation approach (BNWF). This method can be used for both, the nonliquefaction and liquefaction cases. Assembly of a BNWF model requires selection of lateral (*p-y*), axial (*t-z*), and tip bearing (*q-z*) materials for the piles and pile cap. Recommendations regarding the stiffness, ultimate capacity, and nonlinear shape of these curves have been proposed by several authors (Reese et al., 1974; O'Neill & Murchison, 1983; Rollins et al., 2005; Matlock, 1970). More guidance for *p-y* curves selection can be found in the report by Ashford et al. (2011).

Demands from lateral spreading layers can be represented by imposing free-field soil displacements on the free ends of the *p-y* springs of the pile foundation, and also by imposing limit pressures directly to the pile nodes. The imposed free-field soil displacement approach is more general than the limit pressure approach because the latter inherently assumes that soil displacements are large enough to mobilize the ultimate loads from the spreading crust and liquefiable layers against the pile. Brandenberg et al. (2007) performed static pushover analyses of pile groups in liquefied and laterally spreading ground, using the aforementioned approaches. The results of these comparisons indicate that certain guidelines and assumptions, commonly used in engineering design, can produce significantly conservative or unconservative BNWF predictions. For example, not taking into account the structural inertial forces can lead to underprediction of the pile lateral displacements. The authors concluded that although the static BNWF pushover analysis method has limitations, it may be acceptable for design if the uncertainties are recognized and properly accommodated.

In the article by Brandenberg et al. (2012), three bridges supported on deep foundations that exhibited various performance levels in liquefied and laterally spreading ground were analyzed using the BNWF method. These analysis predicted the performance of each bridge quite well when the measured lateral spreading demands were imposed on the bridge. However, these demands were highly uncertain, and different approaches for estimating lateral spreading displacements provided vastly different predictions. Then, these cases were subsequently reanalyzed using a probabilistic prediction. The probabilistic approach provided a rational basis for assessing how much risk is associated with a particular design and provided a superior decision-making framework compared with deterministic methods.

The article by Ledezma (2013) presented back-analyses regarding the seismic performance of the same three bridges selected for analysis in this thesis. The results of the analyzes show that the Youd et al. (2001) liquefaction assessment correlates well with the liquefaction occurrence, and that the calculated liquefaction-induced vertical settlements and lateral displacements, provided realistic estimates of in-situ displacements. It is worth noticing that the back-analyses were performed using an approximate liquefaction threshold. Also, it was assumed that the sliding soil mass, in all cases, behave as a rigid block. This article was used as a starting and comparative point for the results presented in this thesis.

1.4. Methodology

Two methods were used in this study to evaluate the seismic performance of the three selected bridges. The first method can be divided into six phases:

1. Evaluate the liquefaction susceptibility using the SPT profiles from the bridge sites. Two borings from each bridge site where clear evidence of liquefaction was found were selected for evaluation. Liquefaction susceptibility was evaluated using the SPT liquefaction triggering evaluation by Youd et al. (2001).
2. Identify the layers that liquefied along the soil profiles and assign undrained residual strengths to those layers. The undrained residual strength (S_{ur}) is estimated using the expression proposed by Ledezma & Bray (2010).
3. Estimate the maximum lateral ground displacement based in a pseudo-static seismic stability analysis. Knowing the values of the horizontal forces required to reach a factor of safety of 1.0 for the different horizontal accelerations (k_h) and sliding soil mass geometry, the lateral displacement of the soil mass for each k_h is calculated using two earthquake-induced slope displacement models (Bray & Travasarou, 2007; Rathje & Antonakos, 2011) and a sliding block analysis performed in SLAMMER (Jibson et al., 2013).

   The initial fundamental period of the sliding mass (T_s) is required to perform the lateral displacement estimates. The expression used to calculate these values depends on the shear wave velocity (V_s) of the sliding mass, which was estimated using correlations between V_s and $N\text{-}SPT$ values. (Bellana, 2009; Anastasiadis et al., 2002).
4. Identify the most probable plastic mechanism that develops in the pile foundation.
5. Estimate the shear force capacity of the piles against lateral displacement. A pushover analysis was performed using the software LPile (Ensoft, 2013). All models considered

an equivalent single-pile geometry using the same soil layers defined in the slope stability models. Four different types of *p-y* curves (Reese et al., 1974; O'Neill & Murchison, 1983; Rollins et al., 2005; Matlock, 1970) were used to model both liquefiable and non-liquefiable layers, around the pile. Recommendations for scaling factors, p-multipliers m_p, by (Ashford et al., 2011) were used to account for liquefaction occurrence.

6. Stablish a range of possible solutions for the compatible force-displacement state of the foundation and the sliding block solution.

The second method is a probabilistic one with three main phases:

1. Estimate the earthquake intensity at the site of interest of each bridge. Two parameters are used for this purpose, the moment magnitude (M_w) and the spectral acceleration ($S_a(1.5T_s)$) at the degraded period T_s of the sliding mass.
2. Based on the liquefaction triggering evaluation, the slope stability models, and the foundation characteristics, input parameters for the Ledezma & Bray (2010) spreadsheet are selected. The potential base area (A) of the sliding mass is estimated from the slope stability model and the shear force provided by the piles is estimated using the following foundation parameters: pile's Young modulus (E_s), moment of inertia (I_p), length of the pile in the liquefied layer (H), number of piles (N), pile's plastic bending moment (M_y), and pile radius (R).
3. The probability values for five different damage levels are calculated.

1.5. Thesis Structure

This thesis is divided into five chapters:

Chapter 1 is the introduction of the thesis, a brief background explanation of the natural phenomenon that motivated this work is presented. The objectives of this research, a review of the state of the art, and methodology description, are also presented in this chapter.

Chapter 2 corresponds to the article written based on this research, which is the main section of this document. It contains the description of the used procedure, the results obtained for each of the three selected bridges, comparisons of the results obtained from the analytical and probabilistic methods, and conclusions about the differences and similarities between these two methods.

In Chapter 3, a detailed discussion of the final results is made. A comparison between the two methods and the importance and contribution of this research are explained.

Chapter 4 presents the principal conclusions of this research.

Chapter 5 proposes ideas for future work.

2. SIMPLIFIED PROBABILISTIC EVALUATION OF THE SEISMIC PERFORMANCE OF THREE PILE-SUPPORTED BRIDGES AFFECTED BY LIQUEFACTION DURING THE M8.8 MAULE CHILE EARTHQUAKE

Abstract

The 2010 M8.8 Maule Chile earthquake showed that the interaction between liquefied and laterally spreading ground and structures with deep foundations is still far from being completely understood. Damage and partial collapse observed in bridges like Juan Pablo II and Llacolén, was most likely due to the effects of liquefaction-induced lateral and vertical ground displacement, which often cause large ground deformations that impose additional loads on the pile foundations. This article presents a simplified back-analysis regarding the seismic performance of three bridges. The cases are analyzed using two approaches, a liquefaction triggering evaluation along with the pile-pinning concept, and a performance-based probabilistic approach. Reasonable to good agreement between these estimates and the actual seismic behavior of these bridges was found. The bridges were selected because clear evidence of liquefaction was observed at their respective locations. Also, their seismic performance was very different, ranging from little to moderate foundation deformations, causing small to large distributed damage.

2.1. Introduction

In February 27, 2010 the M_w = 8.8 Maule earthquake caused significant damage in Chile's infrastructure. The affected infrastructure spanned a large area of approximately 600 km along the coast, by 100 km wide. This area included several regions and the metropolitan area. The two largest and most populated cities in Chile, Santiago and Concepción, were located in the mentioned area. There is an important highway network that runs in the north-south direction, which connects these two cities, being Route 5 the most important. In this article, three case histories of bridges investigated by the Geotechnical Extreme Events Reconnaissance (GEER) teams during several visits after the earthquake are presented. The observations provided herein are based on the edited GEER report (Bray & Frost, 2010) and on the article by Ledezma et al. (2012).

Two of the three bridges presented in this article cross the Bío-Bío River, which is the second longest river in Chile. It is also the widest river in Chile, with an average width of 1 km, and a width of more than 2 km prior to discharging into the ocean. Close to the Pacific Ocean, the river traverses the metropolitan area of Concepción, Chile's second largest metropolitan area. In Concepción, the river is crossed by five bridges. Concepción was selected as the main area of interest because clear evidence of liquefaction was observed, due to its short distance to the epicenter R$\approx$100 km (62 miles), and to the different seismic performance of Llacolén Bridge (opened in 2000) and Juan Pablo II Bridge (1974). The third bridge that was analyzed is the Mataquito Bridge (2006), located near Iloca, to the north of the epicenter area, which was also subjected to extensive lateral spreading effects due to liquefaction.

Liquefaction triggering and its consequences such as lateral spreading, ground settlement, and approach fill deformations, caused damages that affected the bridges' decks and superstructure, leading to closure, compromising local transportation, and causing logistical problems to treat the emergency. Due to the Maule earthquake the three bridges experienced different levels of structural damage. The most common geotechnical failure mechanism was liquefaction-induced lateral spreading that occurred along both shores of the Bío-Bío and Mataquito rivers.

2.2. Liquefaction Susceptibility

Liquefaction susceptibility was evaluated at the three bridge sites using the Standard Penetration Test (SPT) profiles obtained before and after the earthquake, which were provided by the Ministry of Public Works (MOP in Spanish). The sand liquefaction triggering procedure known as the "simplified procedure" (Youd et al., 2001) was used to define an approximate normalized SPT threshold value for the occurrence of liquefaction. The 2010 Maule earthquake had a moment magnitude of M_w = 8.8, and the ground motion in the

Concepcion area, R≈100 km (62 miles) from the epicenter, had a peak ground acceleration of PGA≈0.4g (Boroschek et al., 2010).

2.3. Liquefaction Effects

Effects of liquefaction-induced lateral spreading were evaluated based on the simplified design procedure proposed in the MCEER/ATC-49-1 report, a guideline for the seismic design of bridges (ATC/MCEER Joint Venture, 2003), where the "pile-pinning" effect was standardized. Some of the principal steps involved in this design procedure are:

- Identify the soil layers that are likely to liquefy. Borings located near the area of interest for each bridge (abutments and/or bents) were selected and evaluated according to the Youd et al. (2001) liquefaction triggering procedure.
- Assign undrained residual shear strengths (S_{ur}) to the layers that liquefy. Once the liquefiable soil layers are identified, the post-liquefaction strength was evaluated using an expression based on a weighted average of five different procedures to estimate the S_{ur} (Ledezma & Bray, 2010).
- Perform pseudo-static seismic stability analyses to calculate the yield coefficient (k_y) for the critical potential sliding mass. For all the analyzed cases, the horizontal force required to reach a factor of safety (FS) of 1.0, defined as P, was calculated for horizontal accelerations k_h of 0.05, 0.10, 0.15, 0.20, 0.25, 0.30, and 0.35. Therefore k_y = k_h since FS = 1.0.
- Estimate the maximum lateral ground displacement. The Bray & Travasarou (2007) relationship and the one proposed by Rathje & Antonakos (2011), along with the software SLAMMER (Jibson et al., 2013), were used to estimate the residual lateral displacement. The initial fundamental period of the sliding mass (T_s) was estimated using the expression: $T_s = 4H/V_s$, where H = the average height of the potential sliding mass, and V_s is the average shear wave velocity of the sliding mass. Shear wave velocities were estimated using V_s versus N-SPT correlations (Bellana, 2009; Anastasiadis et al., 2002).

- Identify the plastic mechanism that is likely to develop in the pile foundation as the ground displaces laterally. A simple elasto-plastic model was used to reproduce the pile behavior.
- From an analysis of the pile response to the liquefaction-induced ground displacement field, the likely shear resistance of the foundation is estimated. Pushover analyses were performed for this purpose using the software LPile (Ensoft, 2013). All models considered an equivalent single-pile geometry using the same soil profile properties assumed for the slope stability models. Several models were considered to assess a range of possible solutions for the compatible force-displacement state from the pushover analyses and the slope lateral deformation.

2.4. Estimation of Residual Lateral Ground Displacement

Two earthquake-induced slope displacement models (Bray & Travasarou, 2007; Rathje & Antonakos, 2011) were used to estimate the lateral ground displacement. The Bray & Travasarou (2007) relationship was evaluated using the rigid block and flexible block approaches. The spectral acceleration at the degraded period $S_a(1.5T_s)$ was estimated using a weighted average of the acceleration records from Hualañe and Concepción stations (Boroschek et al., 2010), and the design spectra of the Chilean regulations NCh433:1996 Mod 2009 (INN, 2009) and Decree 61 modification (MINVU, 2011). A coefficient of variation of 0.4 was assumed for the T_s values. The recommended (PGA, PGV) model by Rathje & Antonakos (2011) was evaluated using the mean shaking period T_m, PGA and PGV of the aforementioned acceleration records, and average results are presented in this article. These relationships will be called, respectively, B&T-07 and R&A-11.

A sliding block analysis was also performed using the software SLAMMER (Jibson et al., 2013). A coupled analysis was performed using a damping ratio of 10%, which corresponds to a shear strain that relates, approximately, to a G/G_{max} ratio of 0.5. Additionally, linear-elastic and equivalent-linear soil models were selected, and their average results are presented in this article.

2.5. Pile Response Analysis

Based on the structural drawings provided by MOP, the foundation piles and bent piers were modeled considering a cylindrical compressive strength of f_c' = 25 MPa for the concrete, and yield and ultimate stresses for the steel of f_y = 420 MPa and f_u = 630 MPa, respectively. These nominal properties were respectively modified by factors R_c = 1.3, R_y = 1.2 and R_u = 1.2 to represent the actual in-situ strength of the piles and piers at the time of the earthquake. These factors are based on the ACI 318-08 (American Concrete Institute, 2008) and AISC 341-10 (American Institute of Steel Construction, 2010) recommendations.

To model the soil around the piles, four different *p-y* curve models were used to represent the liquefied layers, and two models were used for the non-liquefied layers. Two different *p-y* curves for sands were used (Reese et al., 1974; O'Neill & Murchison, 1983)) in both, liquefied and non-liquefied layers; one of those curves is included in the API Recommended Practice 2A-WSD (American Petroleum Institute, 2000). In addition to the sand curves, two other *p-y* curves were used in the liquefied layers (Rollins et al., 2005; Matlock, 1970), one of the curves was originally developed for liquefied sand and the other one was developed for soft clays. Recommendations for the scaling factors, or p-multipliers (m_p), by Ashford et al. (2011) were used to account for liquefaction occurrence. Table 2.1 shows the different combinations of *p-y* curves used in this article.

2.6. Probabilistic Analysis Framework

The Ledezma & Bray (2010) simplified probabilistic design framework was used to evaluate the effects of liquefaction-induced lateral spreading on pile foundations of bridge structures. The procedure uses some of the key assumptions involved in the "pile-pinning" effect, which assumes that the piles are fixed against rotation at some distance above and below the liquefiable material. This procedure incorporates primary sources of uncertainty in its formulation, so that it is compatible with the Pacific Earthquake Engineering Research (PEER) Center Performance-Based Earthquake Engineering (PBEE) framework.

Table 2.1: Models and combinations of *p-y* curves used for pile response analysis.

Model	*p-y* curve Liquefied Layers	*p-y* curve Nonliquefied Layers
LS-SR	Liquefied Sand (Rollins et al., 2005)	Sand (Reese et al., 1974)
LS-API	Liquefied Sand (Rollins et al., 2005)	Sand (API, 2000)
SR-SR*	Sand (Reese et al., 1974)	Sand (Reese et al., 1974)
SR-API*	Sand (Reese et al., 1974)	Sand (API, 2000)
API-API*	Sand (API, 2000)	Sand (API, 2000)
APImp20-API	Sand (API, 2000) m_p = 0.20	Sand (API, 2000)
APImp15-API	Sand (API, 2000) m_p = 0.15	Sand (API, 2000)
APImp11-API	Sand (API, 2000) m_p = 0.11	Sand (API, 2000)
SC-SR	Soft Clay (Matlock, 1970)	Sand (Reese et al., 1974)
SC-API	Soft Clay (Matlock, 1970)	Sand (API, 2000)

*For these models, the *p-y* curves for all layers were model as nonliquefied layers.

In this simplified approach, it is assumed that the amount of seismically induced residual lateral displacement at the bridge abutments or bents, has the primary effect on the overall performance of the entire bridge system. Depending on the level of residual lateral displacement calculated at the bridge abutments or bents, it is proposed to consider that the bridge can reach five potential levels of damage (Table 2.2).

Table 2.2: Bridge damage as a function of residual lateral displacement (Ledezma & Bray, 2010)

Seismic Displacements inches (cm)	Damage Level
0 - 1” (0 - 2.54)	Negligible
1” - 4” (2.54 - 10.2)	Small
4” - 20” (10.2 - 50.8)	Moderate
20” - 80” (50.8 - 203.2)	Large
$>$ 80” (203.2)	Collapse

Some preliminary assessments need to be performed before the proposed simplified procedure can be applied. These include the estimation of the earthquake intensity at the site, a liquefaction triggering assessment, and an evaluation of the liquefaction-induced flow failure potential at the site. The authors of this simplified procedure generated an Excel spreadsheet to perform this evaluation, which was used to obtain the results of this article. The Ledezma & Bray (2010) procedure is meant to work as a screening tool to identify bridges where the effects of liquefaction-induced lateral spreading can be important.

2.7. Mataquito Bridge

2.7.1. Liquefaction Evaluation

The Mataquito Bridge is a 320 m-long, 8-span, reinforced concrete structure that crosses the Mataquito River close to the Pacific Ocean. Each abutment of this bridge was supported by two rows of four drilled shafts of circular cross section. The selected borings for liquefaction evaluation were S-1A and S-2A located near the south and north abutment, respectively (Figure 2.1a). The north abutment showed negligible damages, and since the most notable damages were near the south abutment, the presented results are based on the S-1A boring. Boring S-1A showed that the presence of liquefied material was confined to the upper 5 m of the soil deposit (Figure 2.1). Given that the piles' length was $\sim$17 m, approximately two thirds of the piles lengths were well embedded. This probably provided enough vertical and lateral support for the piles to resist the vertical and lateral loads, despite the occurrence of liquefaction at shallow depths. An average value of $(N_1)_{60cs} \approx 9$ blows/ft was estimated for the full depth of the liquefied layer. The S_{ur}/σ'_v ratio for the slope stability model was 0.096, using the Ledezma & Bray (2010) equation.

2.7.2. Slope Stability Analysis

Based on the available geotechnical information, a simple slope stability model (Figure 2.2) of the south abutment was created using the software Slide (Rocscience, 2012). In this model, a 10 meters-high earth fill, with a 3H to 2V slope (typical MOP specification) is underlain by 5 m of liquefiable material, which in turn is underlain by non-liquefiable material. Correlations between N-SPT and friction angle were used to determine the properties of the earth fill and those of the non-liquefiable layer. The unit weight for all the layers were obtained from data of the borings provided by MOP. For the fill material properties of γ = 22 kN/m^3, c' = 0 kPa and ϕ' = 40° were considered. For the non-liquefiable layer the properties were γ = 20 kN/m^3, c' = 0 kPa and ϕ' = 35°, and the unit weight for the liquefiable layer was γ =18 kN/m^3.

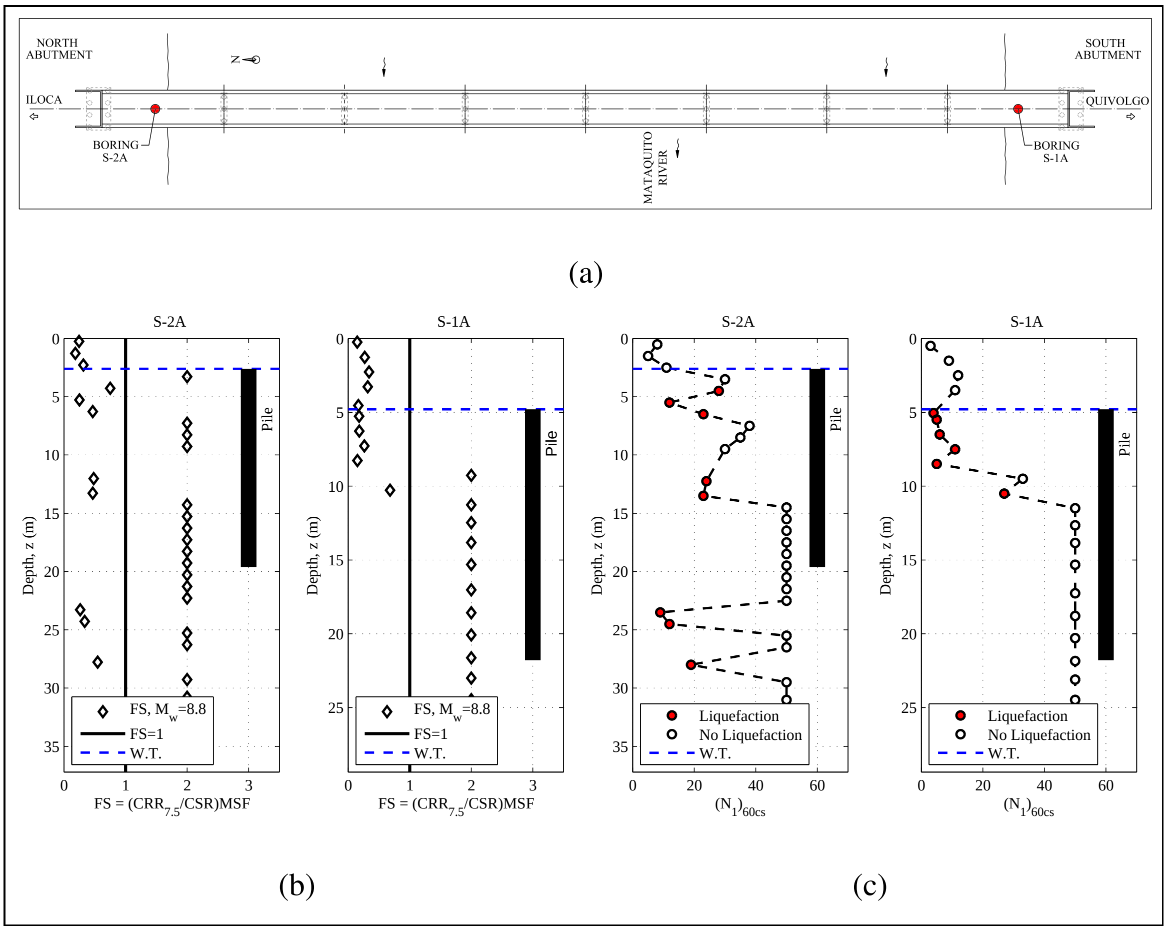

Figure 2.1: (a) Plan view of the Mataquito Bridge, indicating the location of borings S-1A and S-2A; (b) Factor of Safety (FS) against liquefaction occurrence versus depth for moment magnitud M_w = 8.8 and (c) $(N_1)_{60cs}$ profiles indicating liquefiable and non-liquefiable points.

Also, a horizontal force F_{deck} = 377 kN/m, conservatively calculated using Rankine's theory, was included in the analyses to represent the interaction between the abutment wall and the earth fill. This force was located 2H/3 below the earth-fill top, where H is the height of the bridge deck (H = 2.73 m). The horizontal force P required to reach a factor of safety (FS) of 1.0 was located at the center of the liquefiable layer. Then, the B&T-07 and R&A-11 relationships were evaluated, and a sliding block analysis using SLAMMER was performed. The results of these analyses are shown in Figure 2.3. As Figure 2.3 shows, the obtained curves have similar shape regardless of the used method, being the B&T-07 curves the upper and lower boundaries for the set of curves, a pattern that is repeated in the other two bridges.

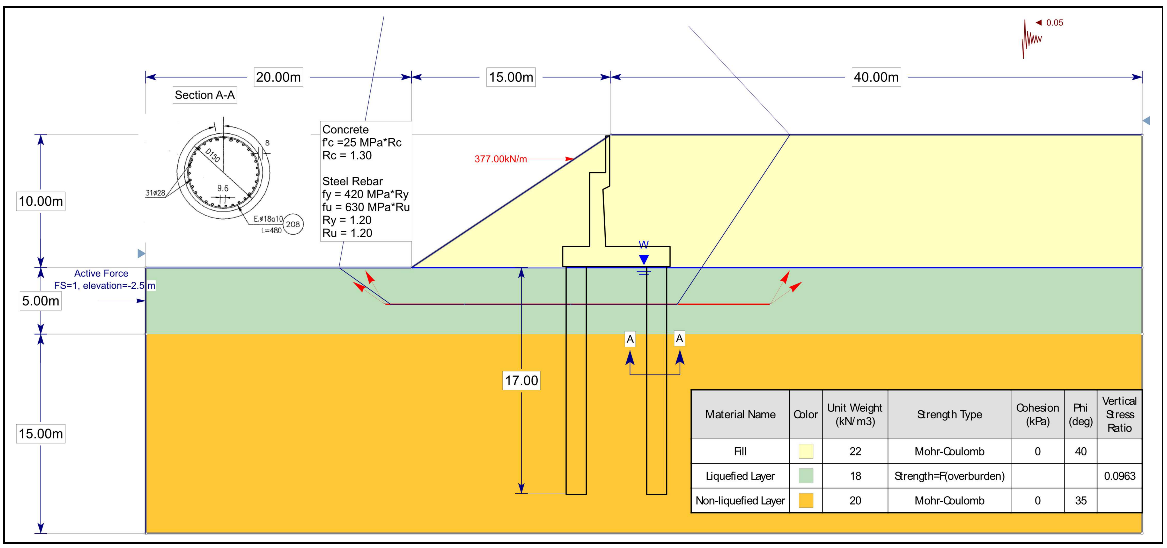

Figure 2.2: Post-liquefaction slope stability model generated for the south abutment of the Mataquito Bridge.

2.7.3. Pile Response Analysis

A pushover analysis of Mataquito Bridge's south abutment was performed considering different p-y curves (see Table 2.1). The model considered an equivalent single-pile geometry and the same soil profile properties assumed in the slope stability model. Given that at each abutment there were two rows of piles along the transverse direction of the bridge, considering a spacing of S = 4 m between piles, and that V is the shear force in the pile, the equivalent per-unit-width force R was estimated as $R = 2V/S$. The results of these analyses is shown in Figure 2.3.

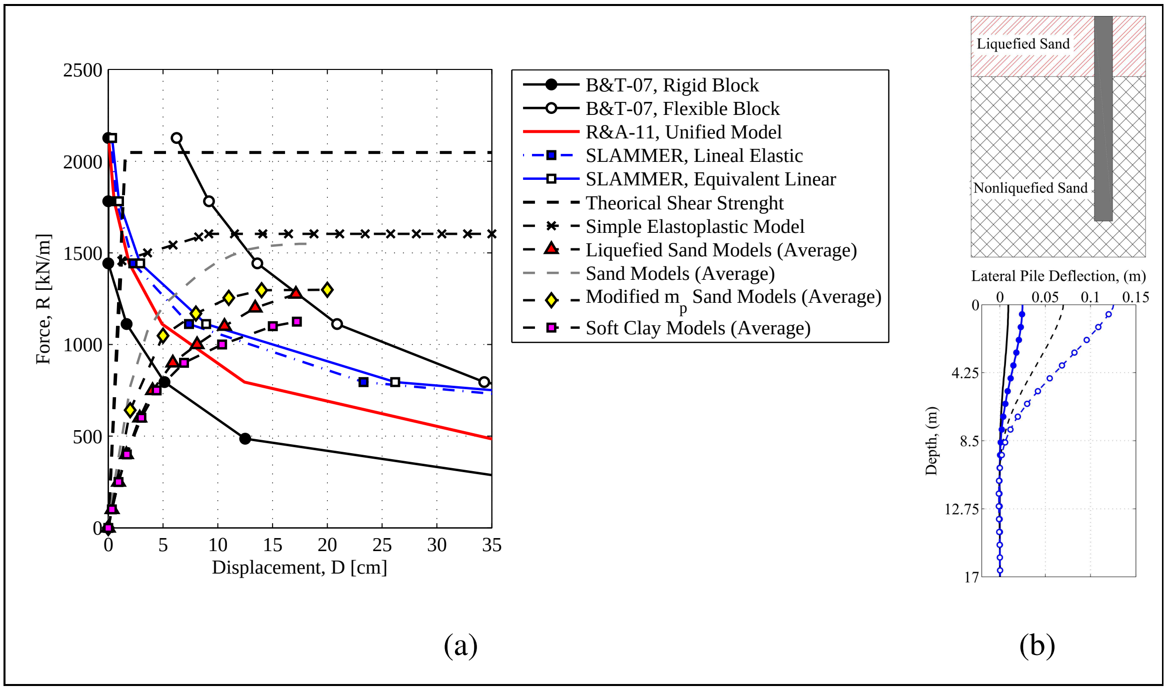

Figure 2.3: (a) Expected lateral displacement D for different values of resisting force R for the piles in the south abutment of Mataquito Bridge. (b) LPile (Ensoft, 2013) equivalent single-pile geometry model and lateral pile deflection for different lateral loads.

This simplified analysis anticipates residual lateral displacement at the south abutment in the range of 4 to 10 cm, but they can be as high as $\sim$18 cm, which is a conservative estimate when compared to what was observed in the field.

2.7.4. Probabilistic Analysis

Using the Ledezma & Bray (2010) spreadsheet, the earthquake intensity at the site is defined through two parameters: the moment magnitude (M_w) of the event, and the spectral acceleration $S_a(1.5T_s)$ at the degraded period T_s of the sliding mass at the location of the bridge. The initial fundamental period (T_s) and the potential base area (A) of the sliding soil mass are obtained from the slope stability analysis (Figure 2.2). Additionally, the procedure uses the shear force provided by the piles defined through the following foundation parameters: pile's Young's modulus (E_s), moment of inertia (I_p), length of pile in the liquefied layer (H), number of piles in the foundation (N), pile's plastic bending moment (M_y) and pile radius (R). Finally, from the liquefaction triggering evaluation, the undrained residual strength (S_{ur}) is estimated. Table 2.3 shows the input data for the Mataquito Bridge.

The α parameter is used to consider the distance to the points of fixity above and below the liquefied layer. Other considerations for this procedure is that the standard deviation of S_{ur} is 0.4 and that the passive reaction force of the bridge deck against the abutment activates after 10.2 cm (4 in) of displacement.

Table 2.3: Input parameters for probabilistic analysis. South abutment of Mataquito Bridge

General Input		Shear Force Input	
M_w	8.8	E_s	23.5 GPa
S_a / $S_a(1.5T_s)$	0.4 g / 0.9 g	I_p	0.245 m^4
T_s	0.12 s	H	5.0 m
A	523 m^2	N	8
S_{ur}	4.20 kPa	M_y	8337 kN-m
α	0.5	R	0.75 m

Figure 2.4 shows that, according to the Ledezma & Bray (2010) simplified procedure, for a rigid block analysis, the probability of having negligible and small damage at the bridge are 81% and 19%, respectively. On the other hand, using a flexible block analysis, the probability values are the same, but now the associated damage levels are small and moderate, respectively.

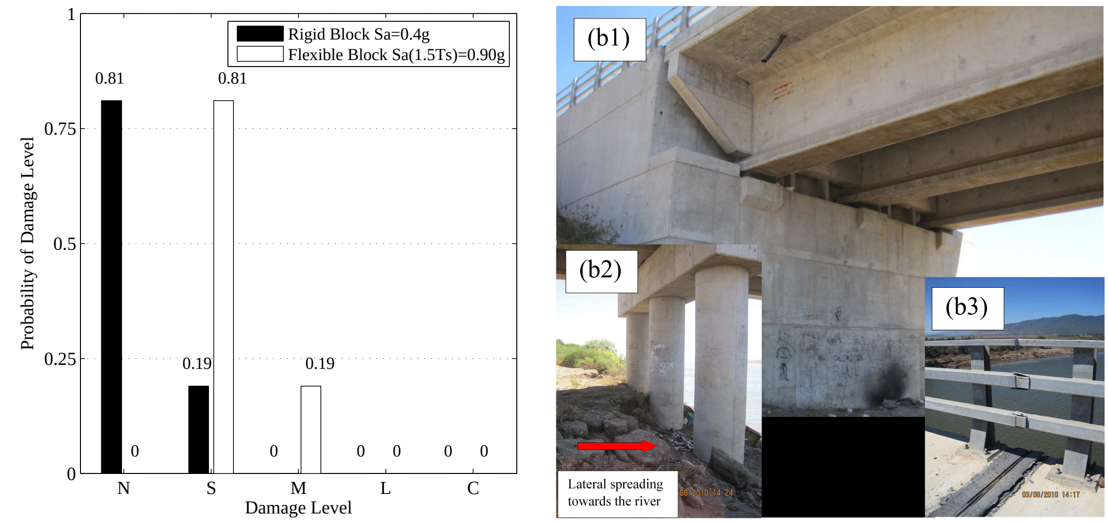

(a) (b)

Figure 2.4: (a) Probability of the south abutment of Mataquito Bridge being in damage levels of negligible (N), small (S), moderate (M), large (L), and collapse (C), as define by Ledezma & Bray (2010), and (b) south abutment of Mataquito Bridge showing no visible damage (b1), signs of lateral spreading on the south end of the bridge (b2), and handrail deformations and overlapping (b3).

2.8. Juan Pablo II Bridge

2.8.1. Liquefaction Evaluation

The Juan Pablo II Bridge is the longest vehicular bridge in Chile, spanning 2,310 m in length. The bridge was opened in 1974. The bridge consists of 70 spans (length = 33 m, width = 21.8 m). Each span sits on reinforced concrete bents with drilled pile supports, piles length was $\sim$16 m. Column shear failure, vertical displacements of the bridge deck, and rotation of the bridge bent of 1° to 3° occurred at the northeast approach. In contrast with the damage observed at the northeast approach, the southwest approach suffered minor damage. The selected borings for liquefaction evaluation were S-14, located near the north abutment and to bent No.66, and S-15, located near the south abutment (Figure 2.5a). Since the bent at Pier No.66 suffered severe damage, the results are based on boring

S-14. Following the procedure used in the Mataquito Bridge, distinct layers of liquefiable material were observed and ours results show that the soil below the tip of the piles likely liquefied during this event. Three liquefied layers were defined, with thicknesses of 6 m, 3 m and 5 m (Figure 2.5). Average values of $(N_1)_{60cs}$ were estimated for the full depth of each liquefied layer. The average $(N_1)_{60cs}$ values were 14, 10, and 12.5 blows/ft. Using the Ledezma & Bray (2010) equation, the S_{ur}/σ'_v ratios for the slope stability model were 0.20, 0.11, and 0.16, respectively.

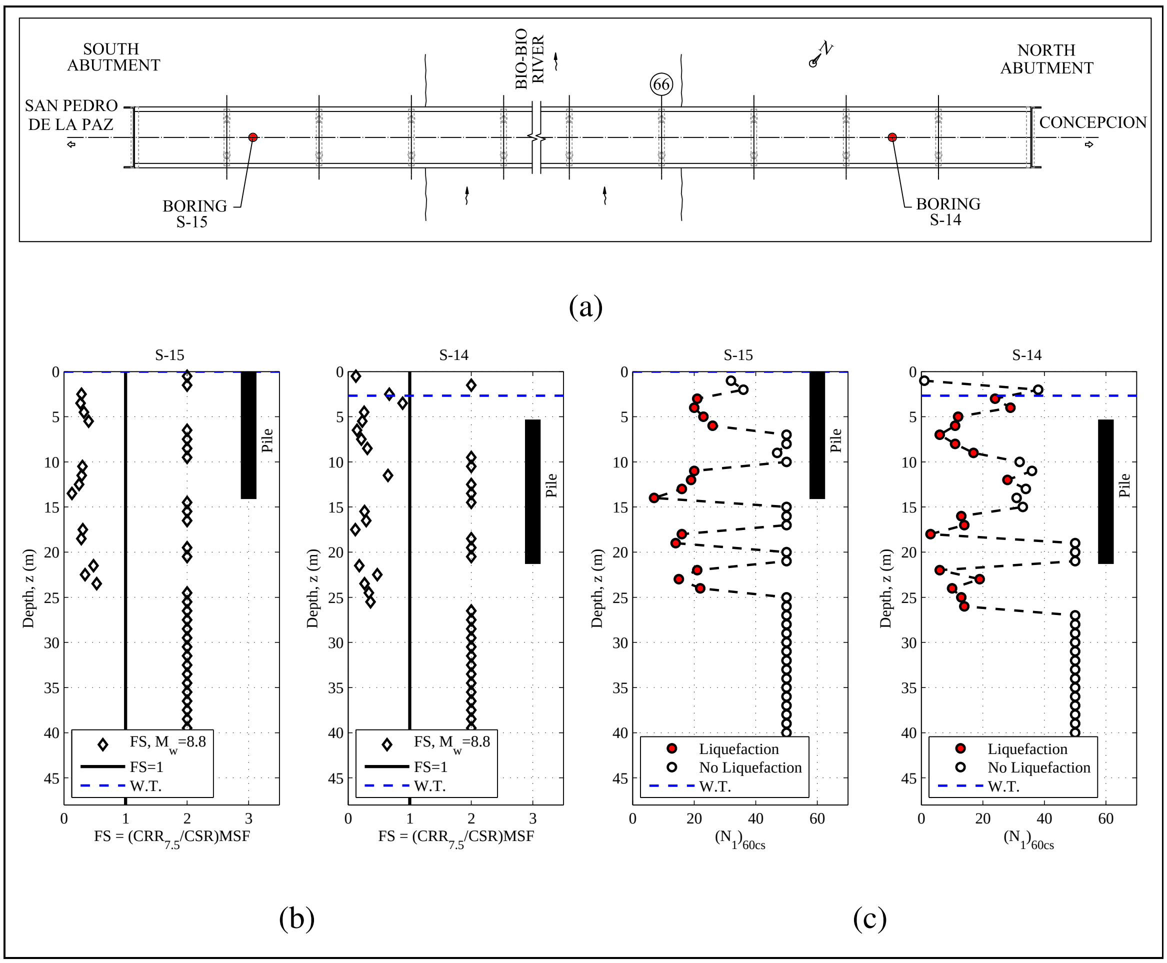

Figure 2.5: (a) Plan view of Juan Pablo II Bridge, indicating the location of borings S-14 and S-15; (b) Factor of Safety (FS) against liquefaction occurrence versus depth for moment magnitude M_w = 8.8, and (c) $(N_1)_{60cs}$ profiles indicating liquefiable and non-liquefiable points.

2.8.2. Slope Stability Analysis

A slope stability model (Figure 2.6) of bent No.66 was created using the software Slide (Rocscience, 2012). In this model, a 6 meters-high earth fill (3H to 2V slope) is underlain by a sequence of liquefiable (L) and nonliquefiable (NL) layers, approximately: top 3 m (earth fill) of NL, then 6 m of L, 7 m of NL, 3 m of L, 3 m of NL, 5 m of L, and NL material for larger depths. For the fill material, properties of γ = 18 kN/m^3, c' = 0 kPa and ϕ' = 28° were considered, for the non-liquefiable layers of medium density the properties were γ = 18.5 kN/m^3, c' = 0 kPa and ϕ' = 30°, and for the dense density layer they were γ = 20 kN/m^3, c' = 0 kPa and ϕ' = 38°. The unit weight for the liquefiable layers was estimated as 19 kN/m^3, 17 kN/m^3, and 17 kN/m^3, respectively. The horizontal force P required to reach a factor of safety (FS) of 1.0 was located at the center of the pile cap. The B&T-07 and R&A-11 relationships, and a SLAMMER model, were used to estimate the residual lateral displacements. The results of these analyses are shown in Figure 2.7.

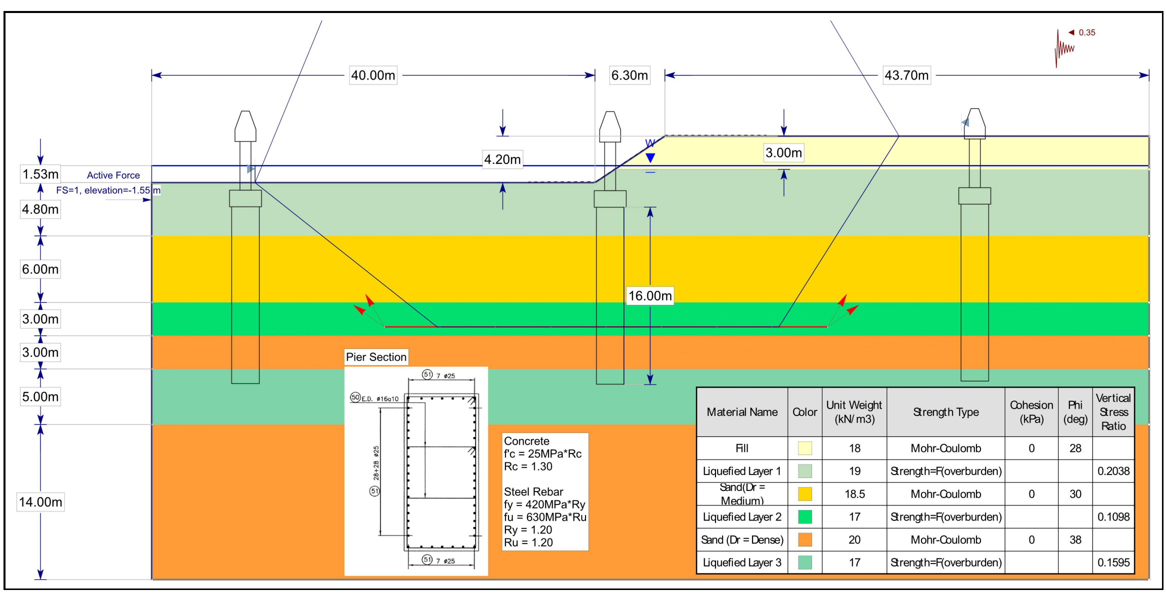

Figure 2.6: Post-liquefaction slope stability model generated for Bent No.66 near the north abutment of Juan Pablo II Bridge.

2.8.3. Pile Response Analysis

A pushover analysis of Juan Pablo II Bridge's No.66 bent pier was performed. Since the shear failure occurred in the pier, and the sequence of liquefiable and non-liquefiable layers did not seem to provide enough lateral restraint, the pushover analysis was focused on the pier rather than on the piles. The model considered an equivalent single pile and column geometry, and the same soil profile properties assumed in the slope stability model. In this case, there was only one row of columns and piles along the transverse direction of the bridge, considering a spacing of S = 13 m between piles, the equivalent per-unit-width force R was estimated as $R = V/S$, were V is the shear force in the pier. The result of this analysis is shown in Figure 2.7.

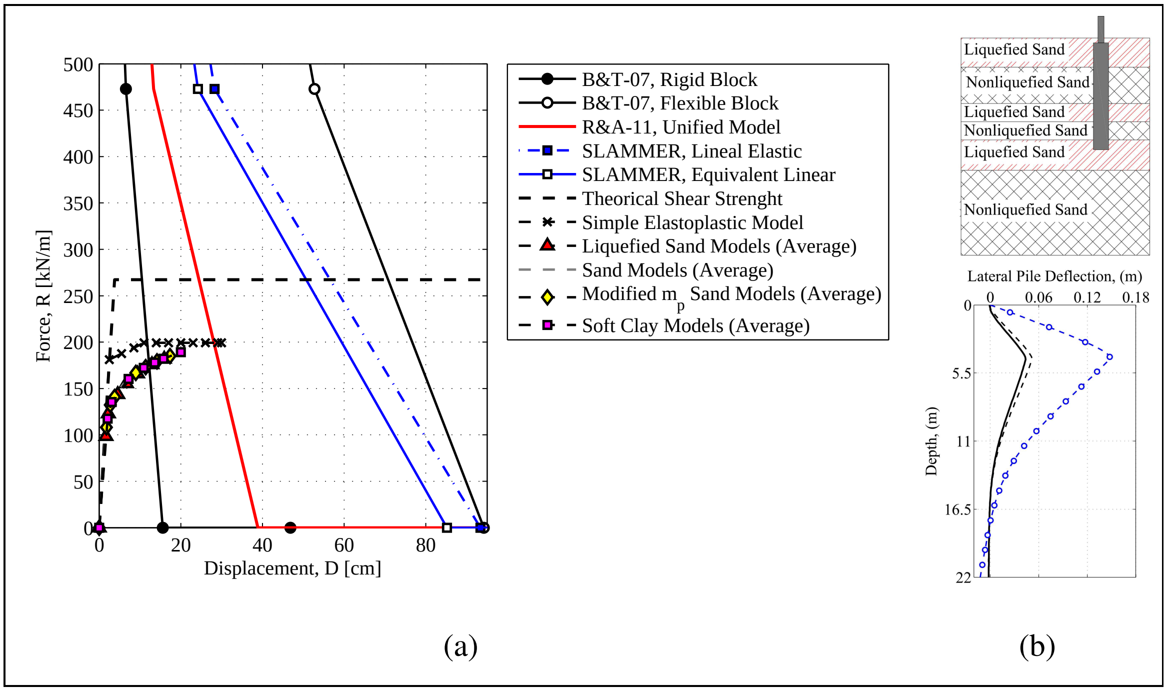

Figure 2.7: (a) Expected lateral displacement D for different values of resisting force R for the piers of Bent No.66 near the north abutment of Juan Pablo II Bridge. (b) LPile (Ensoft, 2013) equivalent single-pile geometry model and lateral pile deflection for different lateral loads.

This simplified analysis shows that the expected lateral displacement at this bent (>10 cm) is consistent with the shear failure of the supporting column observed in the field.

Only one of the ground displacement models intersect the pier response curves, which means that the other models estimate even larger lateral displacements.

2.8.4. Probabilistic Analysis

The input parameters used in the spreadsheet are presented in Table 2.4. The initial fundamental period (T_s) and the potential base area (A) of the sliding soil mass are estimated from the slope stability analysis (Figure 2.6). For this case, since the liquefaction evaluation showed that the soil below the tip of the piles likely liquefied (Figure 2.5), it was assumed that the piles moved along with the soil and that the pier was the only resisting element.

Table 2.4: Input parameters for probabilistic analysis for piers in Bent No.66 of Juan Pablo II Bridge

General Input		Shear Force Input	
M_w	8.8	E_s	23.5 GPa
S_a / $S_a(1.5T_s)$	0.4 g / 1.0 g	I_p	0.175 m^4
T_s	0.26 s	H^*	8.18 m
A	644 m^2	N	2
S_{ur}	15.8 kPa	M_y	18593 kN-m
α	0.0	R^{**}	0.685 m

*Equivalent length of pile, after reformulating the pier restrains.

**Equivalent radius of the rectangular pier section.

This pier-pile system behaved approximately as a vertical cantilever element. Since the Ledezma & Bray (2010) assumes that the lateral resistance comes from piles fixed against rotation above and below the liquefied layer, an equivalent pile element was developed to properly reproduce the pier's lateral stiffness and strength. Using the Ledezma & Bray (2010) simplified procedure, for a rigid block analysis, the probability of having negligible, small, moderate, and large damage at Bent No.66 of Juan Pablo II Bridge are 6%, 56%, 37%, and 1%, respectively. For a flexible block analysis, the damage levels are small, moderate, large, and collapse, with probabilities of 1%, 45%, 51%, and 3%, respectively. The results of this analysis is shown in Figure 2.8.

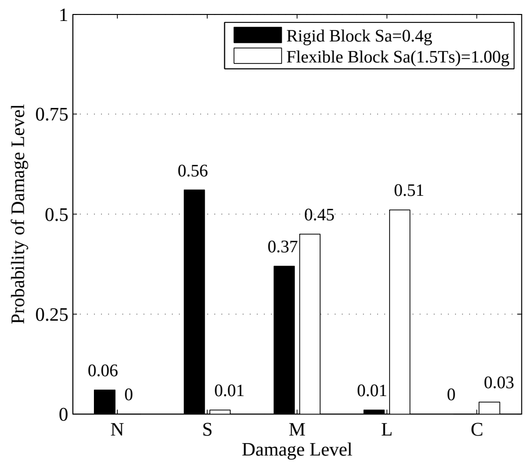

(a)

(b)

Figure 2.8: Probability of the Bent No.66 of Juan Pablo II Bridge being in damage levels of negligible (N), small (S), moderate (M), large (L), and collapse (C), as define by Ledezma & Bray (2010), and (b) Pier shear failure at Bent No.66

2.9. Llacolén Bridge

2.9.1. Liquefaction Evaluation

The Llacolén Bridge in Concepción was constructed in the year 2000 and it spans 2,160 m across the Bío-Bío River. The bridge is a multispan, simply supported concrete girder bridge. In contrast to the Juan Pablo II Bridge, the average piles' length in Llacolén Bridge was ∼20 m. During the earthquake, lateral spreading at the northeast approach unseated the bridge deck at its shoreline support, forcing closure of the bridge until a temporary deck could be erected. The selected borings for liquefaction evaluation were SJ-5 located near the south abutment and S-6 located near the north abutment and to Bent No.48 (Figure 2.9a). The results were most damage was observed are presented (boring S-6). Distinct layers of liquefiable material were observed after the liquefaction evaluation.

Unlike Juan Pablo II Bridge the soil below the tip of the piles did seem to liquefy during this event. Three liquefied layers were defined, with thicknesses of 2 m, 3 m, and 7.5 m (Figure 2.9). Average values of $(N_1)_{60cs}$ were estimated for the full depth of each liquefied layer. The average values were 8.7, 10.8, and 12.5 blows/ft. The calculated S_{ur}/σ'_v ratios, using the Ledezma & Bray (2010) equation were 0.09, 0.13, and 0.23, respectively.

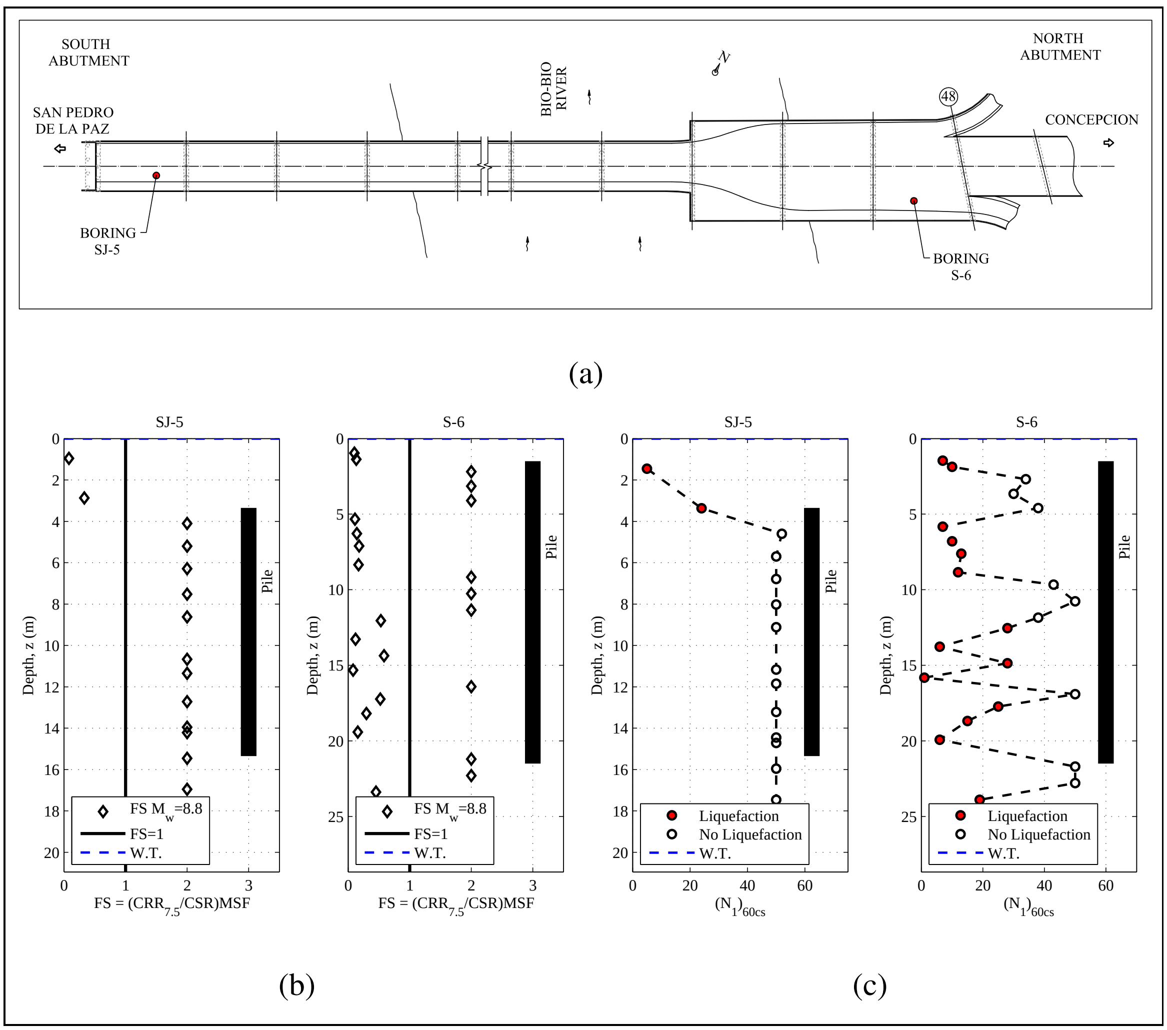

Figure 2.9: (a) Plan view of the Llacolén Bridge, indicating the location of boring SJ-5 and S-6; (b) Factor of Safety (FS) against liquefaction occurrence versus depth for moment magnitude M_w = 8.8, and (c) $(N_1)_{60cs}$ profiles, indicating liquefiable and non-liquefiable points.

2.9.2. Slope Stability Analysis

A slope stability model of Bent No.48 was created (Figure 2.10). In this model, a 3.68 meters-high earth fill (typical 3H to 2V slope) is underlain by a sequence of liquefiable (L) and non-liquefiable (NL) layers, approximately: 2 m of L, 4 m of NL, 3 m of L, 3.5 m of NL, 7.5 m of L, and NL material for larger depths. For the fill, material properties of γ = 22 kN/m^3, c' = 0 kPa and ϕ'= 40° were used. For the non-liquefiable layer of medium density the parameters were γ = 19 kN/m^3, c' = 0 kPa and ϕ' = 30°, and for the dense density layer the properties were γ = 20 kN/m^3, c' = 0 kPa and ϕ' = 33°, the unit weight for the liquefiable layers were estimated as 18.5 kN/m^3, 19 kN/m^3, and 19.5 kN/m^3, respectively. The horizontal force P required to reach a factor of safety (FS) of 1.0 was located at the center of the pile cap. The B&T-07 and R&A-11 relationships, and a SLAMMER model, were again used. The results of these analyses are shown in Figure 2.11.

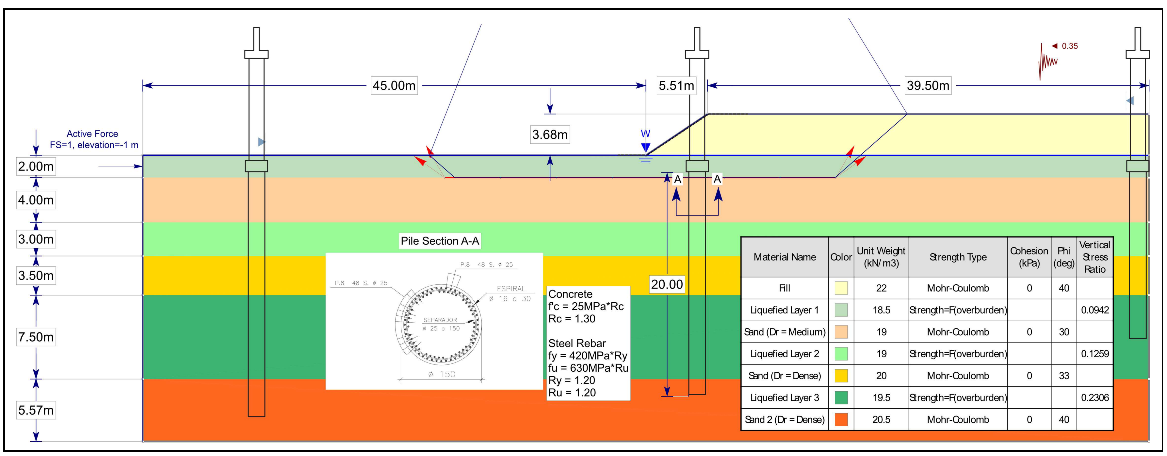

Figure 2.10: Post-liquefaction slope stability model generated for Bent No.48 near the north abutment of the Llacolén Bridge.

2.9.3. Pile Response Analysis

Pushover analyses of Llacolén Bridge's No.48 Bent were performed considering different *p-y* models. It was assumed that the connection of the piers on Bent No.48 to the bridge deck did not provide enough fixity against rotation, so the piles were the only elements restraining the lateral movement of the sliding soil mass. The model considered an equivalent single-pile geometry and the same soil profile properties assumed in the slope stability model. Similar to the Juan Pablo II bridge case, bents had only one row of columns and piles along the transverse direction of the bridge, considering a spacing of S = 4.81 m between piles, the equivalent per-unit-width force R was estimated as $R = V/S$, were V is the shear force in the pile. The result of this analysis is shown in Figure 2.11.

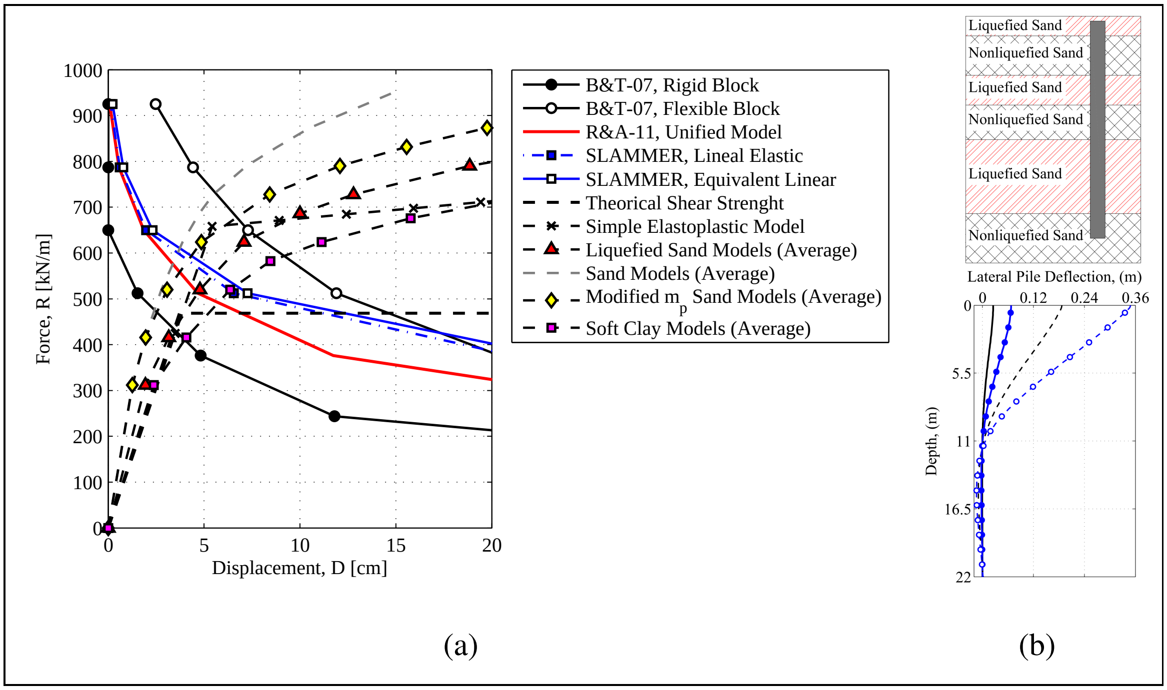

Figure 2.11: (a) Expected lateral displacement D for different values of resisting force R for the piles of Bent No.48 near the north abutment of Llacolén Bridge. (b) LPile (Ensoft, 2013) equivalent single-pile geometry model and lateral pile deflection for different lateral loads.

This simplified analysis shows that the expected residual lateral displacement at this abutment (2 to 8 cm) is consistent with the small to moderate residual lateral displacements observed in the field, which do not fully explain the deck collapse.

2.9.4. Probabilistic Analysis

The input parameters used in the spreadsheet are presented in Table 2.5. The initial fundamental period (T_s) and the potential base area (A) of the sliding soil mass are obtained from the slope stability analysis (Figure 2.10). Even though the failure surface goes through the first liquefied layer of the generated model (Figure 2.10), the pile response analysis showed that the apparent bottom point of fixity of the pile was located between the bottom of the second liquefied layer and the first dense sand layer. Therefore the length of the pile (H) used in this analysis is larger than thickness of the first liquefied layer (Table 2.5).

Table 2.5: Input parameters for probabilistic analysis for Bent No.48 of Llacolén Bridge

General Input		Shear Force Input	
M_w	8.8	E_s	23.5 GPa
S_a / $S_a(1.5T_s)$	0.4 g / 0.72 g	I_p	0.245 m^4
T_s	0.079 s	H	9.0 m
A	1315 m^2	N	10
S_{ur}	5.1 kPa	M_y	13292 kN-m
α	0.83	R	0.75 m

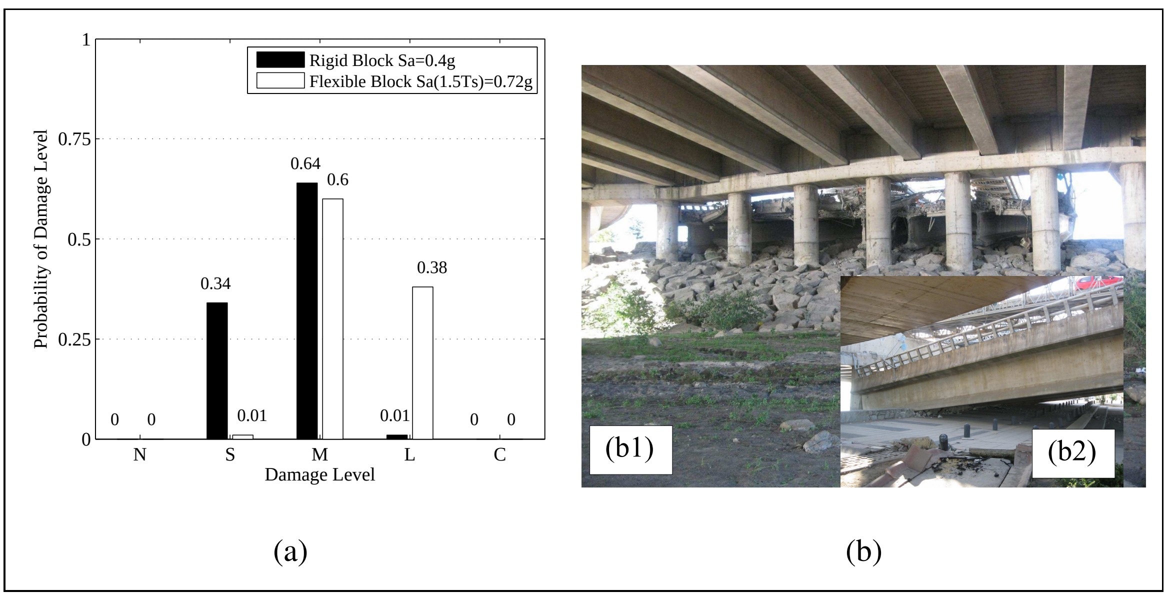

Figure 2.12: (a) Probability of Bent No.48 of Llacolén Bridge being in damage levels of negligible (N), small (S), moderate (M), large (L), and collapse (C), as define by Ledezma & Bray (2010), and (b) substructure of the north approach at Llacolén Bridge showing the unseated deck in the foreground (b1) and north view of the deck unseating at Bent No.48 (b2).

Using the Ledezma & Bray (2010) simplified procedure, for a rigid block analysis, the probability of having small, moderate, and large damage at Bent No.48 of Llacolén Bridge are 34%, 64%, and 1%, respectively. For a flexible block analysis the damage levels are small, moderate, and large, with probability values of 1%, 60%, and 38%, respectively. The result of the analysis is shown in Figure 2.12.

2.10. Conclusions

Assessment of liquefaction susceptibility and liquefaction effects, in terms of lateral spreading, evaluated from SPT-profiles at each bridge site showed that current procedures correlate reasonably well with the observed bridge damage and occurrence of liquefaction at these sites.

The simplified probabilistic method, although conservative, correlate reasonably well with the observed bridge damage, even in the case where a modification had to be made to use the spreadsheet to incorporate the lateral restraining provided by the pier.

In the Mataquito Bridge case, the range of expected lateral displacement was larger than the observed residual displacements on field. The results of the probabilistic method show that the residual lateral displacement using both rigid and flexible block models were consistent (Table 2.6). Results from both methods were conservative.

For the Juan Pablo II Bridge large lateral displacements were estimated, which correlates well with the observed shear failure of the piers (Figure 2.8). Note that equivalent pile properties had to be used in the spreadsheet to represent the columns' lateral response. In the probabilistic method, unlike the other bridges, there was not a specific damage level that stood out from the rest (Figure 2.8). Furthermore, depending on the block model that was used, the damage level could vary from "Small" to "Large", for rigid and flexible block models, respectively (Table 2.6).

For the Llacolén Bridge the residual displacement estimates, using the analytical methods, suggest that lateral spreading may not be the only reason for the bridge deck collapse at the shoreline support, and that inertial effects could have played a relevant role in this case. On the other hand, using the probabilistic method, the bridge deck collapse could be explained because of the conservative range of expected lateral, being the damage level defined as “Moderate” the one with highest probability (Table 2.6).

Table 2.6: Comparison of residual lateral displacement results

Bridge	Residual Lateral Displacement, Analytical Method (cm)	Residual Lateral Displacement, Probabilistic Method (cm)	
		Rigid Block	Flexible Block
Mataquito	4 - 18	0 - 2.5 [81%]	2.5 - 10 [81%]
Juan Pablo II	> 10	2.5 - 10 [56%] 10 - 51 [37%]	10 - 51 [45%] 51 - 203 [51%]
Llacolén	2 - 8	2.5 - 10 [34%] 10 - 51 [64%]	10 - 51 [60%] 51 - 203 [38%]

Acknowledgements

This research was made possible by grants from (i) the Chilean National Commission for Scientific and Technological Research under Fondecyt de Iniciación Award Number 11110125, (ii) the United States Department of State’s Bureau of Educational and Cultural Affairs (ECA) through the Fulbright Program awarded to the author (NEXUS Program), and (iii) the University of Washington’s Visiting Scholarship awarded to the author. Any opinions expressed in this material are those of the authors. Discussions with Prof. Pedro Arduino from the University of Washington, Seattle, were very useful. The authors would also like to thank Carla Serrano, MS student at the Pontificia Universidad Católica de Chile, for compiling the SPT data that was used for this study, and also to the Ministry of Public Works (MOP, Chile) for providing the required data to perform the analyses.

3. ANALYSIS

The results obtained in this research are important for the geotechnical engineering field, because the assessment of liquefaction susceptibility and lateral spreading, evaluated from SPT-profiles, correlate reasonably well with the displacements and damages observed at the studied bridges' abutments and/or bents. Also, because the SPT is still the most used field test for characterization and soil sampling in Chile.

There are various methods to estimate liquefaction induced lateral displacement of structures (e.g., numerical analyses and scale models); however, some of those methods are too complex and computationally costly, hence the importance of having tools that can provide similar estimates but with lower complexity and cost.

There is good agreement between the results of the two analyzed methods and the observed damages in the selected areas of interest, even though the analyses were performed under a pseudo-static assumption (inertial effects from the structure were neglected). The estimated lateral displacements were always on the conservative side, specially with the probabilistic method.

Although the methodology proposed herein achieves of the stated objectives (Chapter 1), some key points were identified.

The first aspect was the determination of the initial fundamental period (T_s) of the sliding soil mass, and the associated spectral acceleration at that degraded period ($S_a(1.5T_s)$), to estimate the residual lateral displacement. These two parameters are key inputs in both Bray & Travasarou (2007), and Rathje & Antonakos (2011) relationships. A commonly used expression is that $T_s = 4H/V_s$, where H is the average height of the potential sliding mass, obtained from the geometry of the slope stability analysis, and V_s is the shear wave velocity, for which no data was available so V_s - N-SPT correlations were used (Bellana, 2009; Anastasiadis et al., 2002). T_s values vary between each other depending on the selected correlation. Taking this variation into account, the $S_a(1.5T_s)$ value for each bridge site was calculated assuming a coefficient of variation of 0.4 for the T_s values. The selected $S_a(1.5T_s)$ values (tables 2.3, 2.4, and 2.5) represent a weighted average for a range of T_s values between $T_s \pm \sigma$, where σ is its standard deviation (Appendix A).

It is worth mentioning that the Rathje & Antonakos (2011) relationship is primarily influenced by the acceleration record used for the analysis, since the input parameters PGA, PGV, and mean shaking period (T_m), are characteristics of each acceleration record. The criteria used to select the acceleration records in this research were: similar record duration, distance to the bridge site, and similarity in the recorded PGA. Selection of more records would have required record scaling, which is beyond the scope of this research.

A second key aspect was detected in the probabilistic method when defining the length of the pile in the liquefiable layer. The spreadsheet was originally developed for a case where *"pinning"* was provided by piles fixed against rotation at some point above and below the liquefied layer: Bent No.66 of Juan Pablo II Bridge did not satisfy this condition. An equivalent pile with the same lateral stiffness and strength of the piers, was used. It is important to note that for this bridge, the structural details of the piles were not available because the bridge was constructed in the early 70s, so nominal properties (provided by MOP) had to be assumed.

A third key point was related to the pile response analysis phase in the case of Juan Pablo II Bridge, where the observed damage served to develop and to verify the assumed structure behavior. The definition of the piles behavior, directly affects the restrictions on the generated pushover analyses. The assumptions used in this investigation proved to be quite accurate, based on the obtained results.

Another relevat point is that the liquefaction triggering procedures (Youd et al., 2001) and the residual lateral displacement procedures (Bray & Travasarou, 2007) were applied even though these procedures were not originally formulated for big magnitude events. For example, the database of the "simplified procedure" (Youd et al., 2001) has only points for M_w below 7.7 and CSR below 0.4, and in the analyzed SPT-profiles there were points that exceeded those limits (appendix B). The Bray & Travasarou (2007) relationship was developed using a database of records with M_w below 7.6 and epicenter distance (R) of less than 100 km, and one of the selected acceleration records is above the limit of the distance to the epicenter. However, both procedures appear to give reliable results despite this observation.

Overall, the proposed methodology can be used as a screening tool to identify bridges where the effects of liquefaction and lateral spreading may be relevant or can compromise the bridge structure.

4. CONCLUSIONS

Current SPT-based procedures to evaluate liquefaction susceptibility and effects due to lateral spreading correlate quite well with the observed occurrence of liquefaction and bridge damage at the selected sites, despite the fact that certain parameters from the liquefaction triggering procedure, were near the limits of the database used to formulate this procedure.

The simplified probabilistic method, although conservative, has a reasonably good correlation with the observed bridge damage, even in the Juan Pablo II Bridge case where the spreadsheet input pile parameters had to be modified to incorporate the lateral restrain provided by the pier.

The probability values in two of the three bridges (figures 2.4 and 2.12) showed one clear damage level, for both rigid and flexible block models, which is an advantage when assessing the expected bridge damage based on the residual lateral displacements.

For the Mataquito Bridge case, the range of expected lateral displacement was larger than the observed residual displacements on field. The results of the probabilistic method show that the residual lateral displacement using both rigid and flexible block models were consistent (table 2.6), also both block models showed a predominant damage level (figure 2.4). Results from both methods were conservative in this case.

For the Juan Pablo II Bridge large lateral displacements were estimated, which correlates well with the observed shear failure of the piers (figure 2.8). Note that equivalent pile properties had to be used in the spreadsheet to represent the pier's lateral response. In the probabilistic method, unlike the other two cases, there was not a specific damage level that stood out of the rest (figure 2.8). Furthermore, depending on the block model that was used, the damage level could vary from small to large, for rigid or flexible block models, respectively.

For the Llacolén Bridge the residual displacement estimates, using the analytical method, suggest that lateral spreading may not be the only reason for the bridge deck collapse at the shoreline support, and that inertial effects could have played a relevant role in this case. On the other hand, the probabilistic method indicates that the bridge deck collapse can be somewhat explained by the lateral displacement, where the damage level defined as “Moderate” had the highest probability (figure 2.12), for both rigid and flexible block models.

Finally, comparing the residual lateral displacement obtained using the analytic and the probabilistic methods, we can conclude that no method is more accurate than the other. While it is true, in the case of the Mataquito Bridge both methods estimate a very similar range of displacement (table 2.6), in the other two cases the range of displacement that most resembles the observed damage is given by the probabilistic method.

5. FUTURE WORK

The proposed methodologies could be used in other bridges in which evidence of liquefaction was found, so as to verify that indeed this tool adequately evaluates liquefaction susceptibility and properly estimates the residual lateral displacement in abutments and/or bents, and to check if these estimates remain in the conservative side. Moreover, projects that are still in a design phase could be analyzed using the available SPT-profiles from the future bridge site, to check the expected lateral displacements and how they could affect the structure.

Another potential line of research is to perform dynamic analyses using numerical models of the bridges discussed in this research, and to compare the results obtained from those models and the results presented in this thesis, to verify whether this simplified evaluation gives reliable results that can help make decisions for improvements and/or changes in the bridge, especially on those projects in a design phase. Moreover, modifications can be made to the Ledezma & Bray (2010) spreadsheet, so other restrain conditions can be evaluated, without the need of formulating an equivalent pile element.

Finally, this procedure could be used as a preventive assessment in those bridges located in areas with high seismic hazard (e.g., northern Chile) in which certain range of displacement may not be tolerable to the structure, causing severe damage to the bridge and logistical problems to attend a potential emergency.

References

American Concrete Institute, . (2008). Building Code Requirements for Structural Concrete (ACI 318-08) and Commentary. Farmington Hills, Michigan.

American Institute of Steel Construction, . (2010). Seismic provisions for structural steel buildings (ANSI/AISC 341-10). Chicago, Illinois.

American Petroleum Institute, . (2000). 2A–WSD Recommended practice for planning, designing and constructing fixed offshore platforms – Working Stress Design. In (21st ed., p. 68-71).

Anastasiadis, A., Raptakis, D., & Pitilakis, K. (2002). Thessaloniki's detailed microzoning: subsurface structure as basis for site response analysis. In *Earthquake microzoning* (pp. 2597–2633). Springer.

Ashford, S. A., Boulanger, R. W., & Brandenberg, S. J. (2011). *Recommended design practice for pile foundations in laterally spreading ground* (PEER Report No. 2011/04). University of California, Berkeley: Pacific Earthquake Engineering Research Center.

ATC/MCEER Joint Venture, . (2003). *Recommended LRFD guidelines for the seismic design of highway bridges* (Liquefaction Study Report No. MCEER/ATC-49-1). Buffalo, New York. (Prepared under NCHRP Project 12-49)

Bellana, N. (2009). Shear wave velocity as function of SPT penetration resistance and vertical effective stress at california bridge sites [Msc thesis]. *University of California, Los Angeles*.

Boroschek, R., Soto, P., & León, R. (2010). *Registros del Terremoto del Maule, Mw=8.8, 27 de Febrero de 2010* (Report No. 10/05). Santiago, Chile: RENADIC.

Brandenberg, S. J., Boulanger, R. W., Kutter, B. L., & Chang, D. (2007). Static pushover analyses of pile groups in liquefied and laterally spreading ground in centrifuge tests. *Journal of Geotechnical and Geoenvironmental Engineering*, *133*(9), 1055–1066.

Brandenberg, S. J., Zhao, M., & Kashighandi, P. (2012). Analysis of three bridges that exhibited various performance levels in liquefied and laterally spreading ground. *Journal* *of Geotechnical and Geoenvironmental Engineering*, *139*(7), 1035–1048.

Bray, J., & Frost, D. (2010). *Geo-engineering Reconnaissance of the 2010 Maule, Chile Earthquake* (Report No. GEER-022 of the NSF Sponsored GEER Association Team). Retrieved from `http://www.geerassociation.org` (Primary Authors: Arduino et al.)

Bray, J., & Travasarou, T. (2007). Simplified procedure for estimating earthquake-induced deviatoric slope displacements. *Journal of Geotechnical and Geoenvironmental Engineering*, *133*(4), 381–392.

Cetin, K. O., Seed, R. B., Der Kiureghian, A., Tokimatsu, K., Harder Jr, L. F., Kayen, R. E., & Moss, R. E. (2004). Standard penetration test-based probabilistic and deterministic assessment of seismic soil liquefaction potential. *Journal of Geotechnical and Geoenvironmental Engineering*, *130*(12), 1314–1340.

Ensoft, I. (2013). *Lpile 2012.6.37* [Computer Software]. Austin, Texas. Retrieved from `http://www.ensoftinc.com`

Idriss, I., & Boulanger, R. (2006). Semi-empirical procedures for evaluating liquefaction potential during earthquakes. *Soil Dynamics and Earthquake Engineering*, *26*(2), 115–130.

INN. (2009). Official Chilean Standard NCh 433 Of. 96 Modificada 2009 " Earthquake Resistant Design of Buildings". (in Spanish). Instituto Nacional de Normalización INN.

Jibson, R. W., Rathje, E. M., Jibson, M. W., & Lee, Y. W. (2013). *Slammer: Seismic landslide movement modeled using earthquake records*. US Department of the Interior, Geological Survey.

Ledezma, C. (2013). Lessons from the seismic performance of pile-supported bridges affected by liquefaction during the M8.8 Maule Chile earthquake. In *Proceedings, 7th international conference in case histories in geotechnical engineering.*

Ledezma, C., & Bray, J. D. (2010). Probabilistic performance-based procedure to evaluate pile foundations at sites with liquefaction-induced lateral displacement. *Journal of geotechnical and geoenvironmental engineering*, *136*(3), 464–476.

Ledezma, C., Hutchinson, T., Ashford, S. A., Moss, R., Arduino, P., Bray, J. D., … others

(2012). Effects of ground failure on bridges, roads, and railroads. *Earthquake Spectra*, *28*(S1), S119–S143.

Marcuson, W. F. (1978). Definition of terms related to liquefaction. *Journal of the Geotechnical Engineering Division*, *104*(9), 1197–1200.

Matlock, H. (1970). Correlation for design of laterally loaded piles in soft clay. In *Proceedings, 2nd offshore technology conference* (Vol. I, p. 577-594).

Medina, C. (2012). *Liquefaction: Fundamentals, Triggering and Consequences* [BGC Engineering Presentation]. Santiago, Chile.

Ministerio de Obras Públicas (MOP). (2010). [Personal cummunication].

MINVU. (2011). DS Nº (61), Reglamento que fija el diseño sísmico de edificios y deroga Decreto Nº 117, de 2010 (in Spanish). Ministerio de Vivienda y Urbanismo. *Diario Oficial*, *13*.

O'Neill, M. W., & Murchison, J. M. (1983). *An evaluation of p-y relationships in sands* (Report to the American Petroleum Institute, PRAC 82-41-1). Houston: University of Houston-University Park.

Phanikanth, V., Choudhury, D., & Reddy, G. (2012). Behavior of single pile in liquefied deposits during earthquakes. *International Journal of Geomechanics*, *13*(4), 454–462.

Rathje, E. M., & Antonakos, G. (2011). A unified model for predicting earthquake-induced sliding displacements of rigid and flexible slopes. *Engineering Geology*, *122*(1), 51–60.

Reese, L. C., Cox, W. R., & Koop, F. D. (1974). Analysis of laterally loaded piles in sand. In *Proceedings, 6th offshore technology conference* (Vol. II, p. 473-484).

Rocscience, I. (2012). *Slide 6.017* [Computer Software]. Toronto, Ontario, Canada. Retrieved from `http://www.rocscience.com`

Rollins, K. M., Gerber, T. M., Lane, J. D., & Ashford, S. A. (2005). Lateral resistance of a full-scale pile group in liquefied sand. *Journal of Geotechnical and Geoenvironmental Engineering*, *131*(1), 115–125.

Seed, H. B., & Idriss, I. M. (1971). Simplified procedure for evaluating soil liquefaction potential. *Journal of the Soil Mechanics and Foundations Division*, *97*(9), 1249–1273.

Verdugo, R., & Peters, G. (2010). *Informe Geotécnico Fase Anteproyecto Infraestructura Puente Mecano Eje Chacabuco* (Rev No. 7).

Youd, T., Idriss, I., Andrus, R. D., Arango, I., Castro, G., Christian, J. T., ... others (2001). Liquefaction resistance of soils: summary report from the 1996 nceer and 1998 nceer/nsf workshops on evaluation of liquefaction resistance of soils. *Journal of Geotechnical and Geoenvironmental Engineering*, *127*(10), 817–833.

APPENDIX

APPENDIX A. SELECTED ACCELERATION RECORDS AND DESIGN SPECTRA

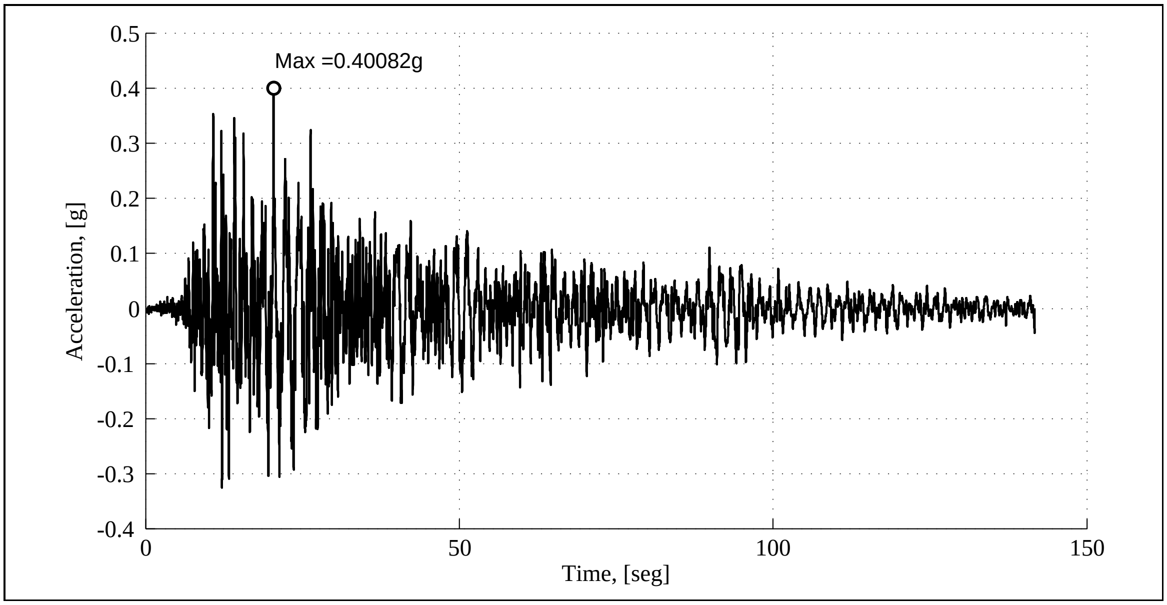

Figure A.1: Acceleration Record of Concepción Station (Boroschek et al., 2010)

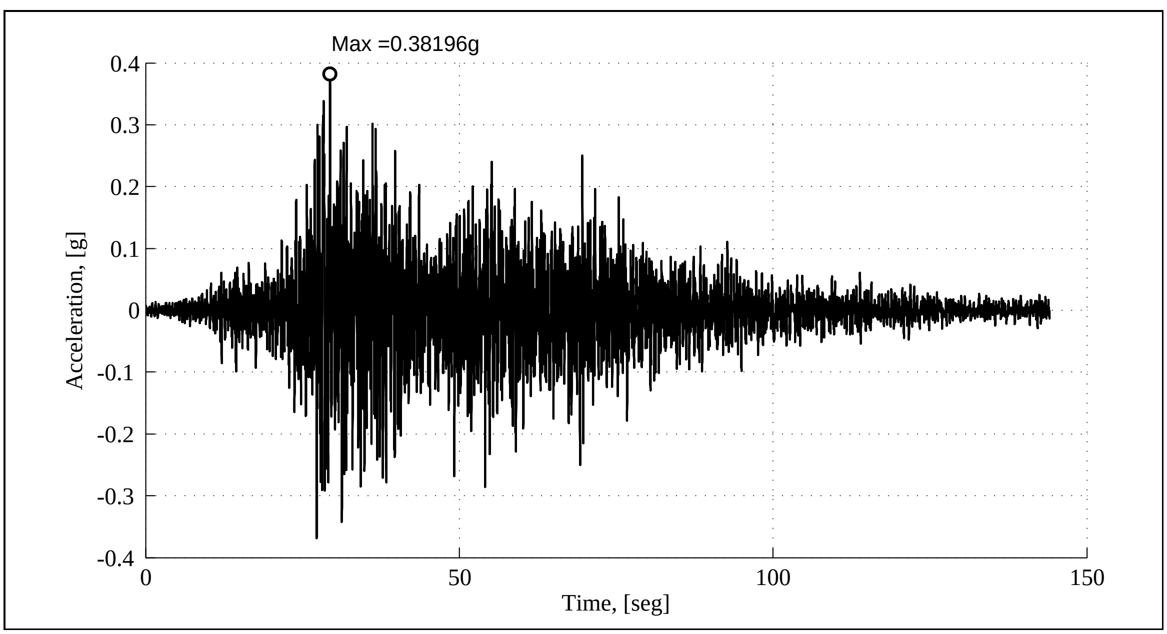

Figure A.2: Acceleration Record of Hualañe Station (Boroschek et al., 2010)

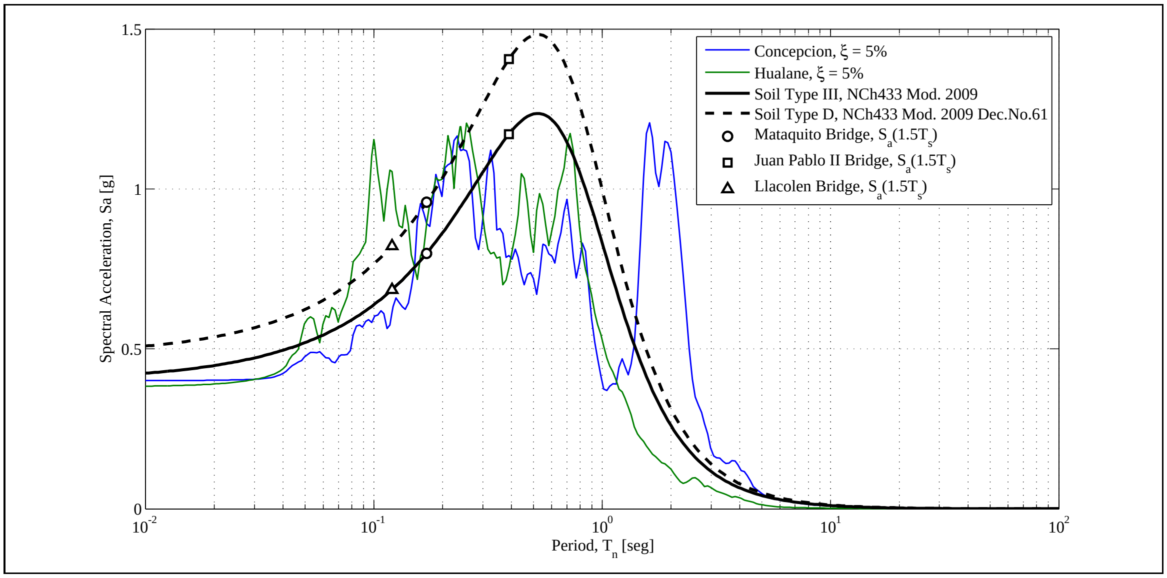

Figure A.3: Response spectra of Concepción and Hualañe records, and design spectra of the Chilean regulations NCh433:1996 Mod 2009 (INN, 2009) and Decree 61 modification (MINVU, 2011)

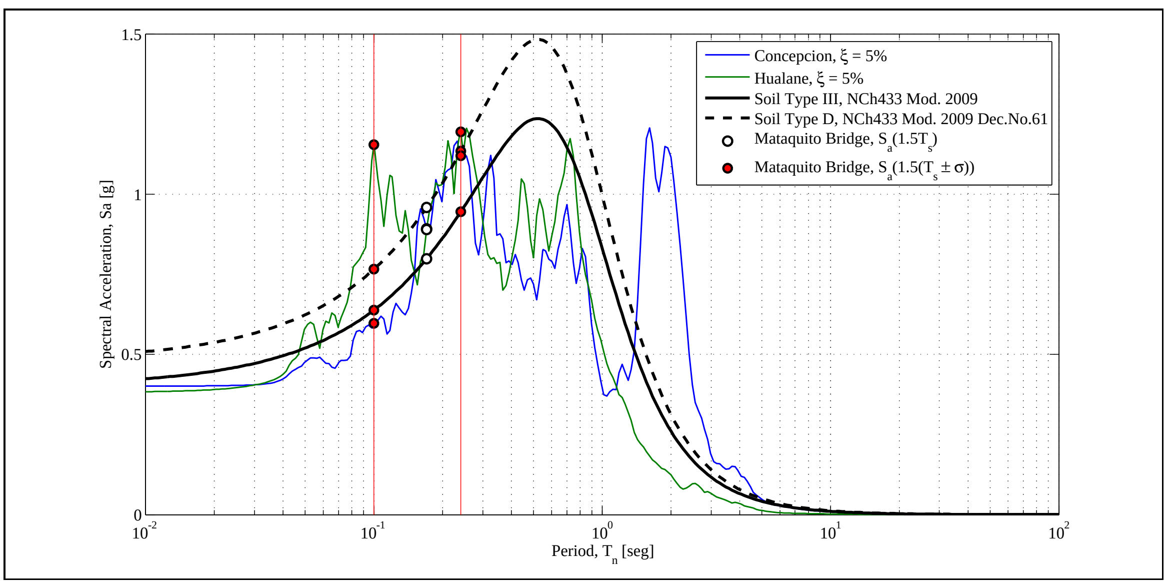

Figure A.4: Range of $S_a(1.5T_s)$ used in the weighted average of Mataquito Bridge

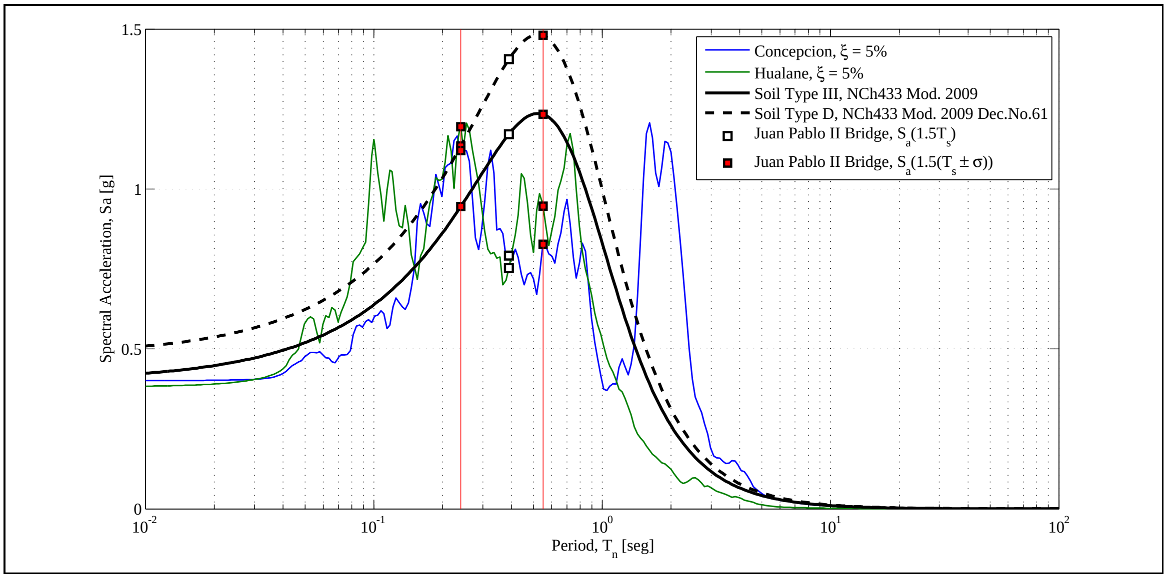

Figure A.5: Range of $S_a(1.5T_s)$ used in the weighted average of Juan Pablo II Bridge

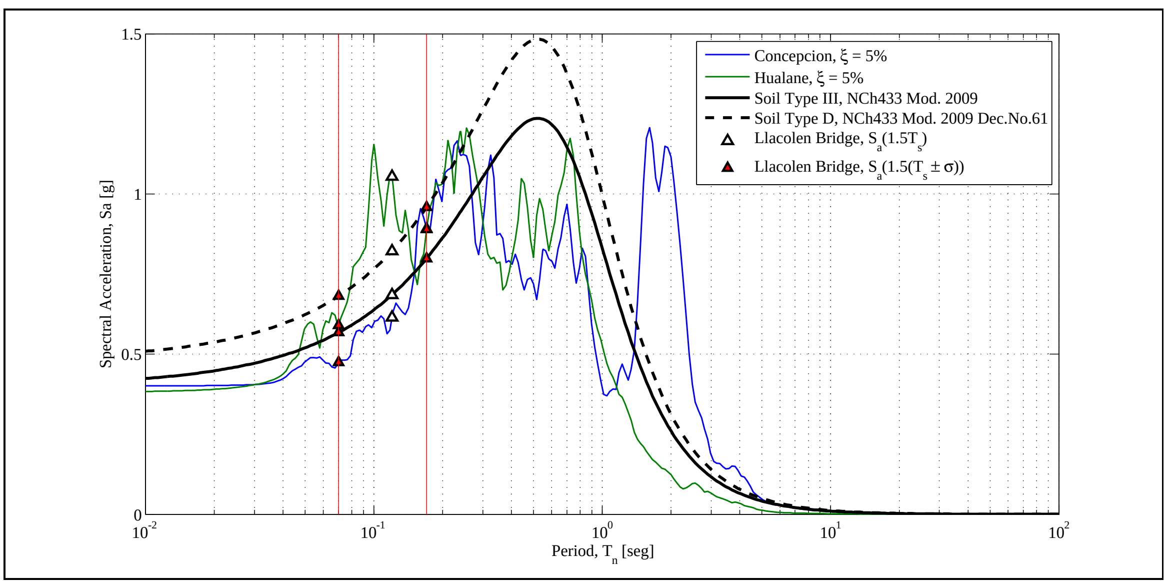

Figure A.6: Range of $S_a(1.5T_s)$ used in the weighted average of Llacolén Bridge

APPENDIX B. FURTHER RESULTS OF LIQUEFACTION SUSCEPTIBILITY

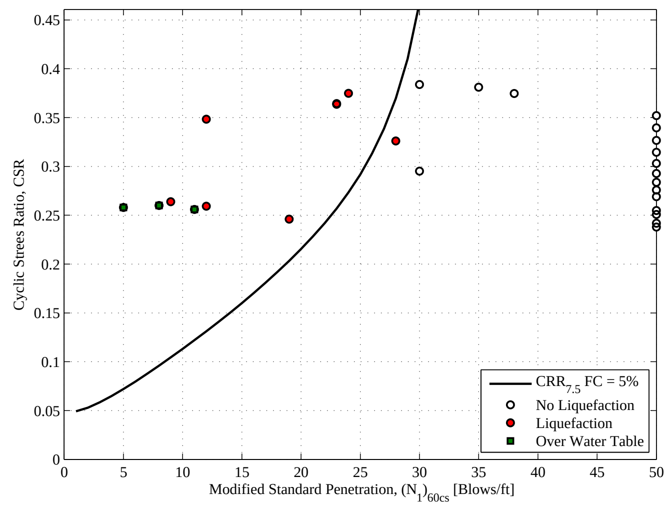

(a)

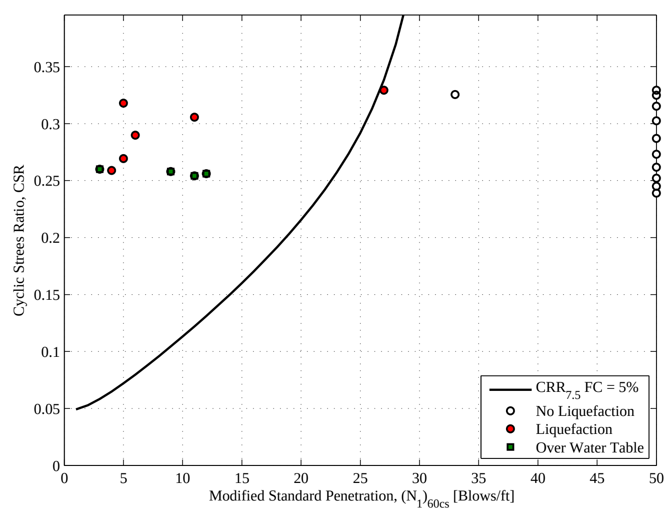

(b)

Figure B.1: Cyclic Stress Ratio (CSR) versus $(N_1)_{60cs}$ and the recommended CRR curve for clean sands, FC = 5%, and M_w = 7.5 (Youd et al., 2001) for Mataquito Bridge; (a) Boring S-2A and (b) Boring S-1A

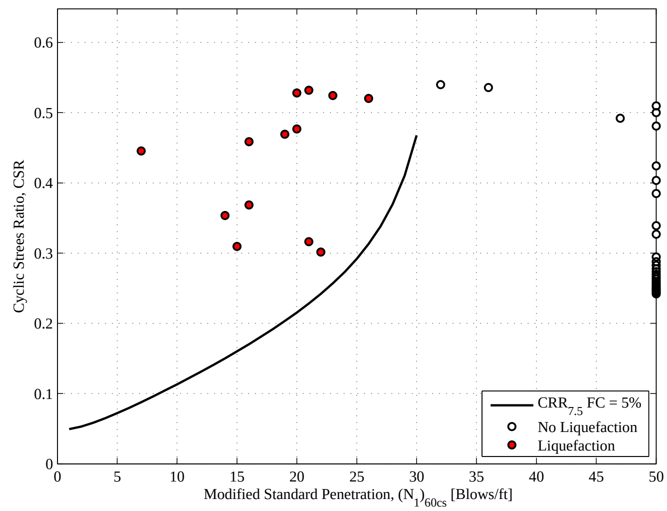

(a)

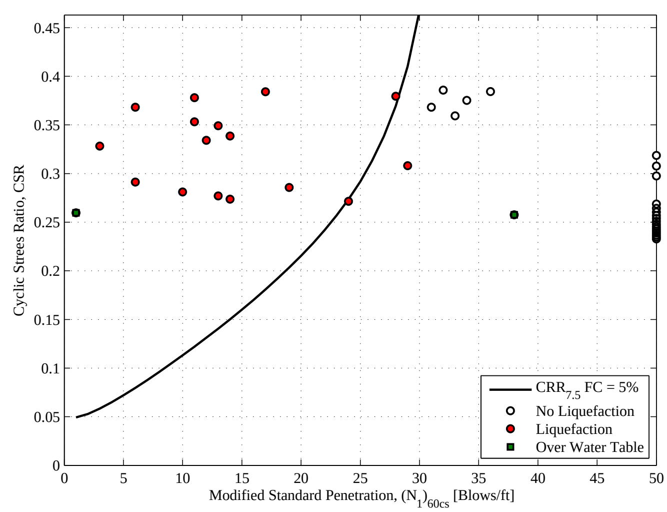

(b)

Figure B.2: Cyclic Stress Ratio (CSR) versus $(N_1)_{60cs}$ and the recommended CRR curve for clean sands, FC = 5%, and M_w = 7.5 (Youd et al., 2001) for Juan Pablo II Bridge; (a) Boring S-15 and (b) Boring S-14

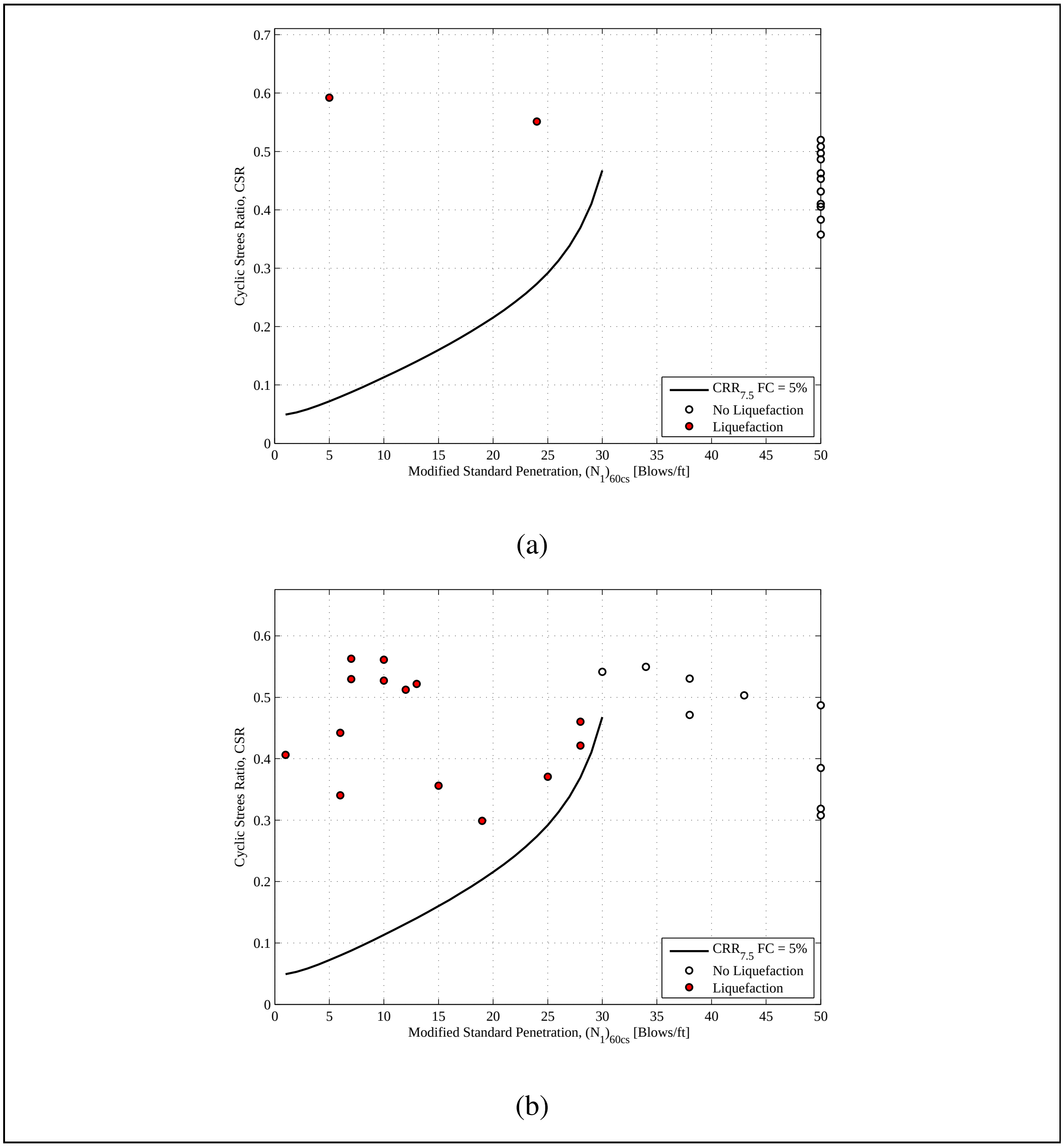

Figure B.3: Cyclic Stress Ratio (CSR) versus $(N_1)_{60cs}$ and the recommended CRR curve for clean sands, FC = 5%, and M_w = 7.5 (Youd et al., 2001) for Llacolén Bridge; (a) Boring SJ-5 and (b) Boring S-6